

Review

Ionic Liquids and Ammoniates as Electrolytes for Advanced Sodium-Based Secondary Batteries

Pablo Hiller-Vallina, Carmen Miralles , Andrés Parra-Puerto  and Roberto Gómez *

Institut Universitari d'Electroquímica i Departament de Química Física, Universitat d'Alacant, Apartat 99, E-03080 Alicante, Spain; pablo.hiller@ua.es (P.H.-V.); carmen.miralles@ua.es (C.M.); andres.parra@ua.es (A.P.-P.)

* Correspondence: roberto.gomez@ua.es

Abstract: This review aims to provide an up-to-date report on the state of the art of electrolytes based on (quasi-)ionic liquids for sodium batteries. Electrolytes based on conventional ionic liquids are classified into one-anion- and two-anion-type electrolytes according to the number of different anions present in the media. Their application for sodium-based batteries is revised, and the potential advantages of two-anion-type electrolytes are highlighted and rationalized based on the higher tunability of interactions among the different electrolyte components enabled by the presence of two different anionic species. Next, the synthesis and properties of liquid ammonia solvates (aka liquid ammoniates) are presented, with a focus on their use as alternative electrolytes. Attention is paid to some of the outstanding properties of ammoniates, notably, their high conductivity and sodium concentrations, together with their ability to sustain dendrite-free sodium deposition, not only on sodium but also on copper collectors. Finally, the prospects and limitations of these electrolytes for the development of new sodium-based batteries, including anode-less devices, are discussed.

Keywords: ammoniates; ionic liquid-based electrolytes; sodium battery electrolytes; dendrite-free deposition; anode-less batteries



Academic Editor: Yuejiao Chen

Received: 23 January 2025

Revised: 6 March 2025

Accepted: 9 March 2025

Published: 9 April 2025

Citation: Hiller-Vallina, P.; Miralles, C.; Parra-Puerto, A.; Gómez, R. Ionic Liquids and Ammoniates as Electrolytes for Advanced Sodium-Based Secondary Batteries. *Batteries* **2025**, *11*, 147. <https://doi.org/10.3390/batteries11040147>

Copyright: © 2025 by the authors. Licensee MDPI, Basel, Switzerland. This article is an open access article distributed under the terms and conditions of the Creative Commons Attribution (CC BY) license (<https://creativecommons.org/licenses/by/4.0/>).

1. Introduction

In the last 20 years, renewable energy has been increasing its presence in the energy landscape, reaching a total of 30% of electricity generation in 2023 [1]. As observed in Figure 1a, the deployment of renewable energies is growing in general, but it varies depending on the geographical region and its available resources. This notwithstanding, fossil fuels are still leading worldwide energy production, with a share of 60.6% (coal and natural gas) in 2023 [2].

The EU, among others, has approved important policies to reduce fossil fuel use and our dependence on it under the EU Green Deal, which highlights a roadmap to be carbon neutral by 2050 [3]. The energy dependence of the EU has been clearly revealed with the high rise in energy prices in recent years. To overcome this problem, the EU published in 2022 the REPowerEU plan to both improve the energy resiliency of the EU and accelerate the clean energy transition [4]. In this respect, the EU made a huge investment in the deployment of renewable energy technologies, and in 2023, the energy production from renewable sources reached 44.7%. The nuclear share in the energy production was 22.8%, while that of fossil fuels decreased by 19.7% down to 32.5% [5]. Solar and wind power are good options for decarbonization due to both their installation versatility and their endless nature. However, as they depend on the weather and the time of the day,

they do not have the versatility of hydropower. In addition, they are dependent on the development of low-cost, efficient, and long-lasting energy storage systems (ESSs) for their proper integration into the energy grid enabling their use at off-peak times. Even when there are different ways to store wind and solar energy [6,7], electrochemical energy storage (EES) systems (batteries) are starting to play a very important role in making them reach their full potential.

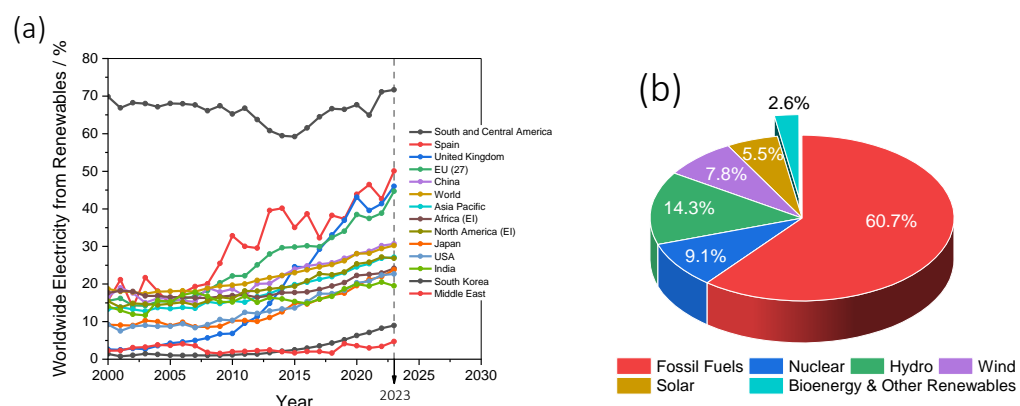


Figure 1. (a) Evolution of renewable electricity production for different countries/regions and sectors. Data obtained from [1]. (b) Worldwide energy production by sources in 2023 [2].

There are many different types of secondary batteries, such as redox flow batteries, nickel-cadmium batteries, lead-carbon batteries, lithium-ion batteries (LIBs), etc. LIBs have been the type of EES experiencing the greatest expansion in recent years. However, for large-scale stationary storage systems, LIBs may not be the best solution due to safety reasons and the requirement of critical raw materials for their fabrication [8]. In this respect, sodium-ion batteries (SIBs) have gained a lot of interest due to their similarity with LIBs and the low cost of sodium (Figure 2), being potentially interesting for the large-scale deployment of stationary storage.

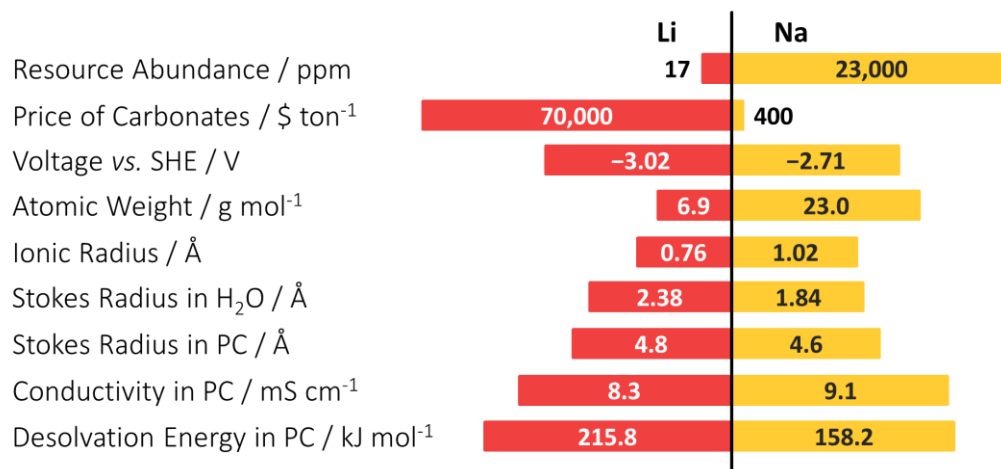


Figure 2. Comparison of the physical and chemical properties of Li and Na. Reproduced with permission [9]. Copyright 2023, Wiley.

Up to now, and in the context of sodium-based batteries, only sodium sulfur (NaS) batteries have been used as large-scale storage systems, thanks to their low cost. However, because of the kinetic limitations of the redox processes, they require high temperatures to run, around 300–350 °C, which, in turn, demands special installations due to safety reasons [8]. The fast development of low-temperature SIBs could bring a more flexible

and safe solution for large-scale energy storage. In 2021, the company CATL announced the first commercial low-temperature SIB [10]. The similarity between LIBs and SIBs is remarkable, as both use liquid electrolytes, and the cathodes are made from analogous raw materials [11]. However, the energy density ranges from 120 to 260 Wh kg⁻¹ for LIBs and from 75 to 160 Wh kg⁻¹ for SIBs [12]. Even with having lower energy densities, the cost reduction in large-scale SIB production can drop from 30 to 40% compared with the lithium iron phosphate (LFP) battery type [13]. A general view of the main differences between LIBs and SIBs is shown in Table 1 [14].

Table 1. Main differences between LIBs and SIBs.

| LIBs | SIBs |
|---|--|
| Larger Li mines are localized in a few countries | Na is more abundant than Li (500 times) and can be extracted from seawater at low cost |
| LIBs require rather high minimum states of charge, raising fire risks in transport | SIBs can be transported fully discharged |
| Anode current collectors are made of Cu, as Li forms alloys with Al at anode potentials | Anode current collector is Al, 3 to 4 times cheaper than copper |
| Low operation temperatures: high risk of fire if operated at high temperature | Higher operational temperatures, without the risk of thermal runaway |
| Relatively slow charge rates and shorter cycle life than SIBs | Faster charging than LIBs with 3 times longer cycle life |

Due to the growing interest in SIBs, work on developments to improve battery performance and avoid critical raw materials is quite intense (an average of 2500 publications per year from 2018 up to now in the Web of Science). The most widely used anode material is carbon in different forms, together with some metal–organic frameworks (MOFs), alloy-forming metals, silicon, TiO₂, etc. [15–18]. Cathodes are based on layered transition metal oxides (LTMOSS), phosphate-based materials, and organic and organometallic compounds (such as Prussian blue and its analogs), among others [19–22]. The most widely used separators are glass fiber-based, polyolefin-based (PVDF, PAN, and PEO), nonwoven-based (cellulose), and polymers with high molecular weight (such as polyamide) [23–26]. Obviously, a critical component of the battery is the electrolyte, on which the focus will be in this review. In the currently dominating organic electrolytes [9,27–29], three components can be identified: sodium salts, organic solvents, and additives [30]. In the following, a short summary of organic electrolytes used in SIBs with their role and ideal properties is provided.

Sodium Salts (Figure 3):

| | |
|------------------|--|
| Role/Impact | <ul style="list-style-type: none"> • Charge transport (electrolyte conductivity) • Stabilization of the solid–electrolyte interface (SEI) • Diffusion of Na ions at the electrode/electrolyte interphase (Na⁺ solvation) • Electrochemical stability window for electrolytes • Corrosiveness and toxicity of sodium salts |
| Ideal Properties | <ul style="list-style-type: none"> • High Solubility (improvement in ion conductivity) • Electrochemical Stability (anion HOMO levels determine positive potential limits while LUMO levels determine SEI formation) • High thermal stability and low toxicity (safe deployment on a large scale) • Chemical stability against other battery components (substrates, current collectors, etc.) |

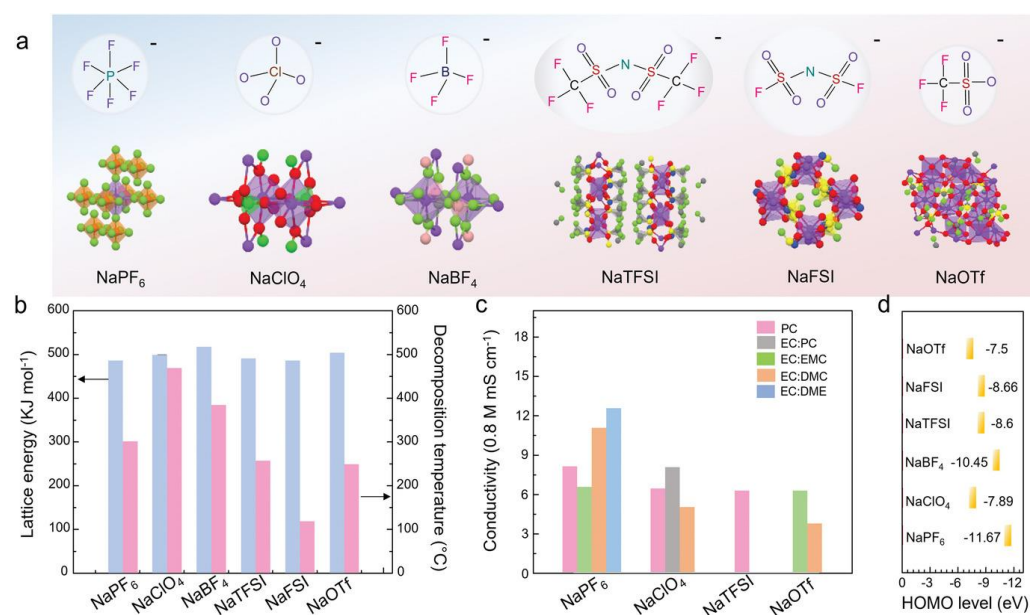


Figure 3. Chemical and physical properties of common sodium salts. (a) Geometric configurations. The 3D structures originate from the Material Project database (Purple: Na; orange: P; red: O; pink: B; blue: N; grey: C; yellow: S; for NaPF₆, NaBF₄, NaTFSI, NaFSI, and NaOTf, green corresponds to F; for NaClO₄, green corresponds to Cl). (b) Lattice energy and decomposition temperature (Arrows indicate the corresponding y-axes). (c) Specific conductivity. (d) HOMO level. Reproduced under terms of the CC-BY license [30]. Copyright 2022, the authors, published by Wiley-VCH.

Organic Solvents (Figure 4):

| |
|---|
| <ul style="list-style-type: none"> • Media for the transport of Na ions • Participation in the formation of a functional SEI • Determination of the solvation structure of Na ions • Modulation of the potential window for the SIBs • Determination of applications based on toxicity and instability (volatility and flammability). |
| <ul style="list-style-type: none"> • High dielectric constant (enhanced conductivity and salt solubility) • Low viscosity (improved ion mobility and conductivity) • Moderate Lewis acid–base nature (Na⁺ coordination; promotion of solvation, enabling de-solvation) |
| <u>Additives:</u> <ul style="list-style-type: none"> • Efficiency improvement by altering the electrode–solution interphase. • Enhancement of electrolyte conductivity by changing Na⁺ solvation and diminishing viscosity/improvement in electrolyte and Na salt stabilities. • Mitigation of other issues, such as overcharging behavior, flammability, and poor low-temperature functionality. |
| <ul style="list-style-type: none"> • As for salts. |

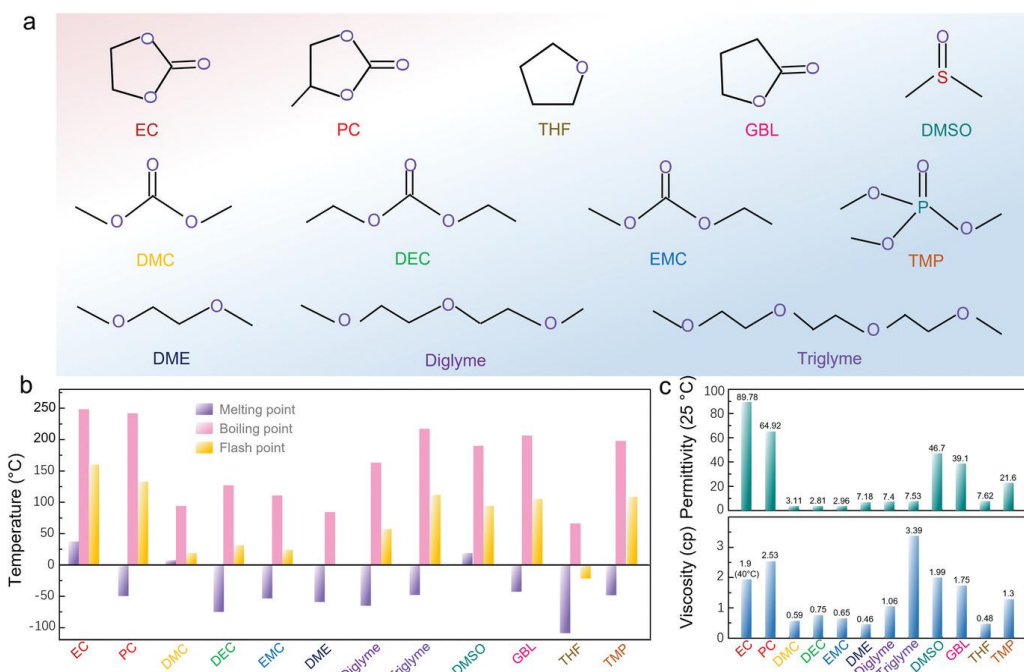


Figure 4. Structure and properties of organic solvents used in SIBs. **(a)** Geometric structure. **(b)** Melting point, boiling point, and flash point. **(c)** Permittivity and viscosity (EC: ethylene carbonate; PC: propylene carbonate, DMC: dimethyl carbonate; DEC: diethyl carbonate; EMC: ethyl methyl carbonate; DME: dimethoxyethane; Diglyme: diethyleneglycol dimethylether; Triglyme: triethylene glycol dimethyl ether; DMSO: dimethyl sulfoxide; GBL: γ -butyrolactone; THF: tetrahydrofuran; TMP: trimethyl phosphate). Reproduced under terms of the CC-BY license [30]. Copyright 2022, the authors, published by Wiley-VCH.

Apart from liquid organic electrolytes, it should be noted that solid-phase electrolytes have recently arisen as a family with high interest due to their fast-charging properties, durability, and safety [28,31–34].

A family of liquid electrolytes attracting considerable interest in recent years is constituted by ionic liquids (ILs). These are pure electrolytes with melting points below 100 $^{\circ}$ C and preferentially liquid under ambient conditions. ILs are either organic salts or inorganic-organic hybrid salts [35,36]. The nature of the ILs gives them unique properties such as high ionic conductivity, excellent thermal, chemical and electrochemical stability, negligible vapor pressure, and high miscibility with other compounds [37]. This review focuses on these electrolytes. Within this family of electrolytes, particular emphasis is placed on the so-called liquid ammoniums, which are ammonia solvates (of sodium salts in the case under scope) characterized by being stable liquids under ambient conditions. They remain largely unexplored for their application in secondary batteries.

2. Ionic Liquids (ILs)

ILs have a history that can be viewed as relatively short. It started in the early 20th century when Paul Walden [38] was exploring the properties of molten salts. He found that $[\text{EtNH}_3][\text{NO}_3]$ had a melting point of 12 $^{\circ}$ C. However, the potential of this breakthrough went unnoticed for a long time [39]. Interest surged in the 1980s [40–44] when researchers recognized their unique characteristics, such as negligible vapor pressure and high thermal stability, making them attractive for various applications in chemistry and engineering. In 1999, Solvent Innovation GmbH began to commercialize ILs with high quality [45]. Since then, ILs have gained attention for their potential in fields like catalysis [46] and electrochemistry [47–49] and as solvents for green chemistry [50]. It was

not until the late 1990s that the application of ILs for rechargeable batteries began to be explored. Gray et al. [51] and Scordilis-Kelleya and Carlin [52] reported reversible Li and Na deposition/stripping using either LiCl or NaCl dissolved in a mixture of 1-methyl-3-ethylimidazolium chloride (MEIC) and aluminum chloride (AlCl_3) as a room-temperature molten salt. Since 2004, the interest in ILs for batteries has experienced intensive growth, as shown by the number of publications in the field that have appeared per year (Figure 5).

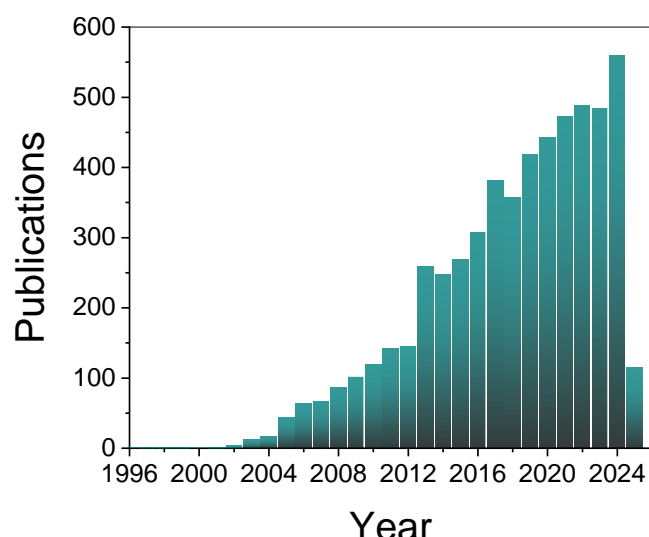


Figure 5. Publications on ILs per year in the context of batteries; data obtained from Scopus (February 2025).

2.1. Classification of ILs

As mentioned above, ILs typically comprise cations and anions of rather different natures, and they have melting points well below 100 °C. These low melting points are due to reduced interionic interactions resulting from their bulky and irregular structures. In contrast, conventional molten salts feature tightly packed, rather symmetrical ions, leading to higher melting points. Their diversity and tunability of ILs derive from the existence of multiple combinations of the typical constituent ions, up to 10^{18} or more [53]. Figure 6 shows the most common ions involved in ILs for battery applications. In this context, an ideal IL should be an electrolyte with high ionic conductivity and high thermal and electrochemical stability.

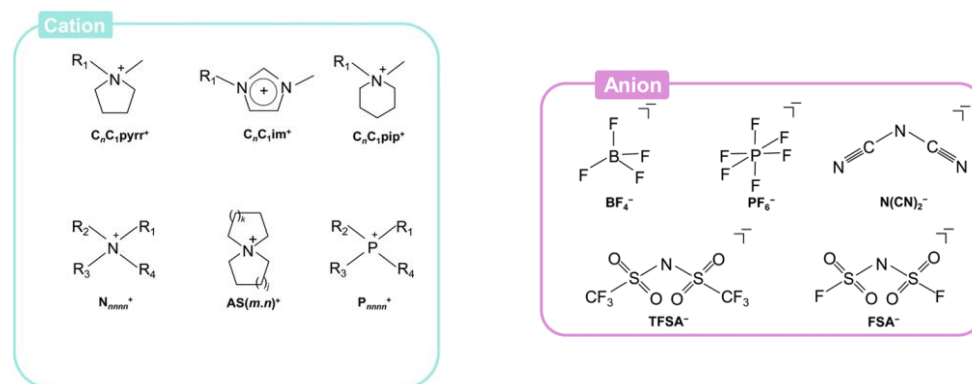


Figure 6. Typical ionic species present in the ILs of interest for secondary battery applications. Cations: $\text{C}_n\text{C}_1\text{im}^+$, $\text{C}_n\text{C}_1\text{pyrr}^+$, $\text{C}_n\text{C}_1\text{pip}^+$, N_{nnnn}^+ , $\text{AS}(m \cdot n)^+$, and P_{nnnn}^+ ; anions: BF_4^- , PF_6^- , $\text{N}(\text{CN})_2^-$, FSA^- , and TFSA^- . Reproduced with permission [54]. Copyright 2019, Royal Society of Chemistry.

ILs can be classified into different groups. One may think of dividing them into protic (PILs) and aprotic (AILs). PILs are characterized by having an available (ionizable) proton in the cation structure, which is not the case for AILs. This introduces an additional source of ion–ion interactions within the structure of the ILs beyond the typical Coulombic and dispersion forces [55]. On the other hand, AILs have been the most widely used ILs due to their superior thermal and electrochemical stabilities. They offer a broad potential window of up to 5 V, which makes them suitable for use in high-voltage batteries [56,57]. However, the synthesis of AILs involves not only multistep processes but also purification processes, making the use of AILs less suitable and less cost-effective for mass production [55,58].

It is worth mentioning that, for a very long time, the use of PILs as battery electrolytes was not considered a feasible strategy due to drawbacks such as reactivity toward the alkali metals and poor electrochemical stability [55,59,60]. However, PILs present less shielded cations. This characteristic is linked to the “cation competition effect”, which leads to increased mobility of the alkaline metal ions in mixtures of PILs and alkaline metal salts. In view of their potential advantages, several researchers have been working to overcome PIL issues. Menne et al. could successfully prevent the reduction of protic cations by including vinyl ethylene carbonate as an additive to the electrolyte [61]. The use of this film-forming additive allows lithium intercalation and deintercalation (near 0 V vs. Li⁺/Li), even when occurring outside the electrochemical stability window of PILs. In 2021, Lingua et al. reported reversible plating and stripping of Li metal using an electrolyte composed of [C₄Hpyrr][TFSI]:LiTFSI (4:1) and 10 wt% of vinylene carbonate [62]. In this case, the use of a SEI-forming additive enables high-performance lithium-metal batteries with LFP and NMC cathodes.

In the context of SIBs, Vogl et al. successfully combined a PIL-based electrolyte and a sodium-ion hybrid device [63]. They claimed that the NaTFSI-[C₄Hpyrr][TFSI] electrolyte offers a specific capacity higher than that of typical AILs. However, this electrolyte faced some cyclability issues when used for studying a layered oxide-based cathode.

2.2. Properties of ILs

As mentioned above, ILs are entirely composed of ions and have emerged as promising candidates for next-generation electrolytes in energy storage devices due to their unique properties. Implementing the use of ILs in SIB research, development, and innovation requires a deep understanding of their physical and chemical properties.

2.2.1. Thermal Stability

Thermal stability is critical for the potential implementation of ILs in SIBs. The operational temperature window of a device is determined by the freezing and boiling points of the electrolyte. The upper temperature limit is a major drawback for traditional organic solvents, which are often based on carbonates with a relatively low boiling point of around 100 °C [28].

Negligible vapor pressure is one of the most celebrated properties of ILs. Due to the electrostatic interactions between the ions in ILs, they typically do not evaporate, which means that their upper temperature limit is usually determined by their decomposition. This is often analyzed by using thermogravimetry (TG) and differential scanning calorimetry (DSC) [64]. For instance, thermogravimetric analysis (TGA) of [C₄C₁pyrr][TFSI] with various sodium salts, such as NaBF₄, NaPF₆, NaClO₄, and NaTFSI, has shown decomposition temperatures in the range of 330 to 400 °C [65]. Similar values have been given for imidazolium-based ILs, with decomposition temperatures ranging from 250 to over 450 °C [66].

Cao et al. [67] investigated the thermal stabilities of 66 ILs, and they concluded that imidazolium-based ILs are generally more stable than tetraalkyl ammonium-, piperidinium-, and pyridinium-based ILs. Furthermore, they reported that stability improves with shorter chain lengths and that the nature of anions is a major factor in establishing thermal stability [67].

2.2.2. Conductivity and Viscosity

The ideal properties of the SIB organic electrolytes shown in Figure 4 also apply to ILs. The performance of ILs in an electrochemical device is influenced by the structure and behavior of their constituent ions. It is vital to ensure a rapid transport of the electroactive species to and from the electrode surface. In this regard, ionic conductivity, diffusion rate, and transport number become relevant.

ILs may have higher ionic conductivities than conventional organic electrolytes at room temperature. Usually, for Na-containing ILs, conductivity values range from 1 to 10 mS cm^{-1} [64], and they increase with temperature. For example, the ionic conductivity of $\text{NaFSI}-[\text{C}_2\text{C}_1\text{im}][\text{FSI}]$ increases from 5.4 mS cm^{-1} at 298 K to 31.1 mS cm^{-1} at 363 K [68]. However, it should be noted that, due to their high viscosity and concentration, ILs possess low molar conductivity at room temperature, resulting from poor ion mobility. In fact, the viscosity of ILs is rather high, from 10 to several 1000 cP , which is well above that of aqueous and organic electrolytes (Figure 4). This results from strong interionic interactions, including van der Waals forces and hydrogen bonding [69]. Specifically, increasing the length of the alkyl chains and introducing fluorine groups enhances viscosity because more extensive and stronger van der Waals interactions and hydrogen bonding are enabled [70].

2.2.3. Electrochemical Stability Window (ESW)

One of the reasons for the recent growing interest in ILs is their wide electrochemical stability window (ESW), which refers to the potential range within which an IL can operate without undergoing decomposition. By carefully selecting the cation and anion structures, as well as by considering temperature effects, ILs with optimal stability can be developed for high-performance applications. ILs offer ESWs as wide as 4–5 V. For example, pyrrolidinium or the ether-functionalized sulfonium families enable operating voltages over 3.5 V [71]. Other studies have revealed that pure ILs with typical fluor oanions have electrochemical windows of 4 to 5 V [72].

The nature of both cations and anions affects the ESW width. Specifically, it has been shown that the structural characteristics of the anion, such as size and charge distribution, can lead to significant differences in the IL electrochemical behavior. In this context, Kazemiabnavi and co-workers [73] calculated by means of the Density Functional Theory (DFT) the electrochemical stability window of a series of $[\text{C}_n\text{C}_1\text{im}]^+$ ILs. They found that highly fluorinated anions, such as $[\text{PF}_6]^-$ and $[\text{BF}_4]^-$, exhibit greater electrochemical stability against reduction and oxidation, which was attributed to the influence of the highly electronegative fluorine atoms, which shift upward the LUMO energy level and downward the HOMO energy level. As for the cation influence, for example, Mousavi et al. [74] studied IL common cations, such as pyridinium, saturated quaternary ammonium, and imidazolium cation. Saturated cations with quaternary ammonium substituents generally make them more resistant to reduction, providing the best cathodic stabilities. In contrast, aromatic cations are less stable due to their lower LUMO energy levels. ILs exhibit different stabilities based on their alkyl side chains. Several researchers reported an improvement in the electrochemical stability of $[\text{C}_n\text{C}_1\text{im}][\text{TFSI}]$ [75] and $[\text{C}_n\text{C}_1\text{pyr}][\text{TFSI}]$ [76] by increasing the chain length of the alkyl substituents. However, the same structural change has been reported to decrease the ESW in the case of $[\text{C}_n\text{C}_n\text{pip}][\text{TFSI}]$ [77].

Other aspects to be considered are the effect of high operation temperatures [78] and the water presence [79], which tend to narrow the ESW. For instance, Randström et al. [80] reported that the addition of 800 ppm of water drastically reduces the cathodic stability of $[C_4C_1\text{pyr}][\text{TFSI}]$. Table 2 summarizes the ESW width for common ILs.

Table 2. Physicochemical and electrochemical properties for common ionic liquids (data taken from IoLiTec Ionic Liquids Technologies unless otherwise specified).

| Ionic Liquid | Tm (°C) | MW (g mol ⁻¹) | Decomp. Temperature (°C) | η (cp) at 25 °C | σ (mS cm ⁻¹) at 25 °C | ESW (V) |
|-------------------------------------|---------|---------------------------|--------------------------|-----------------|-----------------------------------|----------|
| $[C_4C_1\text{im}][\text{TFSI}]$ | -4 | 419.36 | 425 [67] | 48.8 | 3.41 | 3.41 |
| $[C_4C_1\text{im}][\text{FSI}]$ | - | 319.35 | - | 34.8 | 1.04 | 4.7 |
| $[C_4C_1\text{im}][\text{SCN}]$ | -47 | 197.30 | <300 [67] | 35.9 | 8.98 (30 °C) | - |
| $[C_4C_1\text{im}][\text{BF}_4]$ | -83 | 226.02 | 400 [31] | 103 | 3.15 | 4.9 |
| $[C_4C_1\text{im}][\text{PF}_6]$ | -8 | 284.18 | 420 [67] | 310 | 1.92 | 4.0 |
| $[C_4C_1\text{im}][\text{DCA}]$ | -6 | 205.26 | - | 28 | 9.53 | - |
| $[C_2C_1\text{im}][\text{TFSI}]$ | -17 | 391.3 | 420 | 39.4 (20 °C) | 6.63 (20 °C) | 4.7 |
| $[C_2C_1\text{im}][\text{FSI}]$ | -23 | 291.3 | - | - | 6.176 | 4.54 |
| $[C_2C_1\text{im}][\text{BF}_4]$ | 15 | 197.97 | ~415 [67] | ~42 [81] | ~15 [81] | 6.9 [73] |
| $[C_2C_1\text{im}][\text{DCA}]$ | -21 | 177.21 | - | 16.8 | 25.3 | 3.0 |
| $[C_2C_1\text{im}][\text{SCN}]$ | -6 | 169.25 | <300 [67] | 24.7 | 17.8 | 3.2 |
| $[C_2C_1\text{im}][\text{OTf}]$ | -10 | 260.23 | ~400 [31] | 24.9 [81] | 8.8 [81] | 4.7 [73] |
| $[C_4C_1\text{pyrr}][\text{TFSI}]$ | -18 | 422.41 | ~400 [65] | 94.4 | 2.0 | 5.3 |
| $[C_4C_1\text{pyrr}][\text{FSI}]$ | -19 | 322.39 | - | - | - | 5 [81] |
| $[C_4C_1\text{pyrr}][\text{DCA}]$ | -55 | 208.30 | - | 46 (20 °C) | 3.25 (24 °C) | 3.5 |
| $[C_3C_1\text{pyrr}][\text{TFSI}]$ | 12 | 408.4 | 498 [82] | 58.7 | 4.92 (30 °C) | 5.9 |
| $[C_3C_1\text{pyrr}][\text{FSI}]$ | -9 | - | - | - | - | 5.4 [81] |
| $[\text{N}_{2,1,1,3}][\text{TFSI}]$ | 0 | 396.37 | - | 69 | 2.67 | - |
| $[\text{N}_{2,2,2,5}][\text{TFSI}]$ | 3 | 452.5 | - | 93.5 | 1.08 | - |
| $[\text{N}_{4441}][\text{FSI}]$ | 19 | 380.51 | - | 45.5 | 4.33 | 5.7 |
| $[\text{N}_{1114}][\text{TFSI}]$ | 7 | 396.37 | - | 99.5 | 2.86 | 6.1 |

2.3. ILs in Sodium-Based Batteries

As shown in Figure 5, the number of studies on ILs as electrolytes in batteries has been increasing in recent years. In fact, ILs have advantageous properties even when compared with the carbonate and ether electrolytes currently applied in commercial Li-ion and Na-ion batteries [83]. Nonetheless, ILs have the disadvantage of their relatively high cost. In this section, the use of ILs as stand-alone electrolytes in sodium-based batteries will be reviewed, with a focus on anode and cathode performance and SEI formation.

The tunability of ILs derives from the uncountable different combinations of constituent cations and anions. For their use as SIB electrolytes in large-scale EES applications, they need to have the properties mentioned above, namely, low viscosity, high ionic conductivity, wide ESW, non-hazardous components, low flammability, and high thermal stability, together with cost-effective electrolyte synthesis. Another important characteristic of the electrolyte is its ability to form a uniform and stable SEI, which can be described as a passivating film on top of the electrode (positive or negative) resulting from electrolyte decomposition and/or reaction with the electrode material. The film formed on the negative electrode is called the SEI, while at the positive electrode, it is also known as a cathode–electrolyte interface (CEI). The SEI comprises inorganic and organic components depending on the electrolyte decomposition products. To ensure good electrochemical cell performance, the SEI layer must be stable, flexible, uniform, electronically insulating, and suitably thick. It has been demonstrated that the presence of organic components provides flexibility, while the presence of inorganic components confers high ionic conductivity. In the organic electrolytes commonly used for SIBs, the SEI layer tends to dissolve upon cycling, which results in poor Coulombic efficiency in comparison with the LIB SEIs, whose solubility is lower [84,85].

The stability and features of the SEIs depend on the type of organic electrolyte employed. In ether-type solvents, the generated SEI film is more uniform and thinner and contains more inorganic compounds than in carbonate-type solvents. In addition, ether-based electrolytes are less reactive against Na metal than carbonate-based electrolytes [86]. Some inorganic compounds that have been identified in SEIs are Na_2O , NaF , and Na_2CO_3 as well as organic compounds like RONa , ROCO_2Na , and RCOONa (R = alkyl group) [87–89]. In the case of ILs, the SEI structure and composition also depend on the nature of IL cations and anions as well as on the anion of the metal salt. Owing to the tunable composition of ILs, the properties of the generated SEI can be set to the benefit of the electrochemical performance by choosing the appropriate combinations of cations and anions. Tunability is one of the greatest advantages of using ILs as electrolytes against conventional organic electrolytes [90]. However, there is a lack of knowledge about the formation of SEIs in ILs due to difficulties related to the study of the interface in this case. In the literature, there is a relatively large number of reports in which the SEI formation mechanism and composition are detailed for ILs.

In the context of SIBs, IL-based electrolytes are composed of a sodium salt dissolved in an IL. The addition of sodium salt tends to increase the density, the glass transition temperature (T_g), and the viscosity of ILs and to decrease their ionic conductivity because of an increment of interionic interactions. The typical sodium salts used in ILs are those used for organic solvents [91] (see Figure 3). NaPF_6 is used as the benchmark salt for SIBs in organic solvents owing to the weak interaction between Na^+ and PF_6^- , which promotes sodium salt dissociation and decreases the formation of ionic pairs [92]. However, in the presence of water, NaPF_6 suffers hydrolysis to yield harmful products (HF , PF_5 , and POF_3) [93]. NaTFSI and NaFSI salts have safety features superior to those of NaPF_6 because they have higher thermal stability and less toxicity [93]. Both are frequently applied to IL-based electrolytes for SIBs.

Although tunability resulting from a wide composition choice has been mentioned as one of the advantages of ILs, it is somewhat limited by the choice of anions, as just a few of them lead to practical electrolytes. The choice of cations is wider, and one may find among those commonly used imidazolium, pyrrolidinium, pyrazolium, pyridinium, piperidinium, morpholinium, ammonium, and phosphonium. The physical properties of the ILs will strongly depend on the nature of their constituent cations [94]. It is known that the introduction of long substituent groups decreases the thermal stability and increases the viscosity of ILs. Therefore, short alkyl chains are desired in general. On the other hand, it is observed that the use of imidazolium cations, with an acidic proton, is limited because of their low stability [95]. In general, AILs are more suitable for sodium batteries than PILs. Imidazolium-based ILs have lower chemical stability than pyrrolidinium ones as they have several reactive sites in their structure. The ESWs for imidazolium-based ILs thus tend to be narrower [96–98]. In contrast, pyrrolidinium-based ILs are the most investigated ones in the context of SIBs because they have wider ESWs. We may classify the IL-based electrolytes for SIBs according to the number of different anions present in the system (Figure 7), that is, depending on the existence in the electrolyte of either one type of anion (the Na salt and IL anions are the same) or two types of anions (the Na salt and IL anions are different from each other).

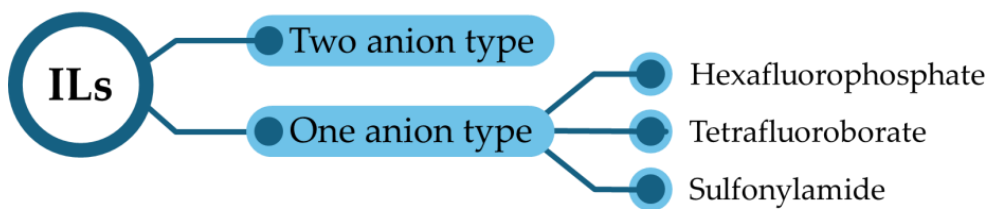


Figure 7. Scheme of a classification of IL-based electrolytes for SIBs according to the number of different anions present in the system.

2.3.1. One-Anion-Type Electrolytes

One-anion-type electrolytes for SIBs can be divided into three groups according to the nature of the anion: (i) hexafluorophosphate-based $\text{NaPF}_6\text{-}[X^+]\text{[PF}_6^-]$, (ii) tetrafluoroborate-based $\text{NaBF}_4\text{-}[X^+]\text{[BF}_4^-]$, and (iii) sulfonylamide-based electrolytes $\text{NaTFSI}\text{-}[X^+]\text{[TFSI}^-]$ and $\text{NaFSI}\text{-}[X^+]\text{[FSI}^-]$. These types of IL-based electrolytes contain fluorinated anions owing to their relative facile synthesis and their ability to support stable SEIs. The main drawbacks of using these fluorine-based electrolytes are their high viscosity and high cost. The ionic conductivity and the viscosity of the electrolytes are influenced by the sodium salt concentration. When it increases, the ionic conductivity decreases, and the viscosity increases. In any case, high transport numbers for sodium ions have been observed for super-concentrated IL-based electrolytes. Actually, the electrochemical behavior of Na^+ ions is more influenced by the transport mechanism at the electrode than by the overall ionic conductivity of the electrolyte [99,100].

$\text{NaPF}_6\text{-}[X^+]\text{[PF}_6^-]$ -Based Electrolytes

The number of different ionic liquids comprising PF_6^- anions is limited because there are only a few combinations with cations that yield ILs with melting points below room temperature [101]. The reason behind this is the nature of hexafluorophosphate, characterized by high rigidity and by being highly symmetrical. The IL-based electrolytes formed by NaPF_6 and an $[X^+]\text{[PF}_6^-]$ ionic liquid have low stability against hydrolysis and high viscosities, which hinders their use in battery applications [102,103].

$\text{NaBF}_4\text{-}[X^+]\text{[BF}_4^-]$ -Based Electrolytes

They have lower melting points and a slightly higher water tolerance than electrolytes containing the PF_6^- anion. However, the synthesis of tetrafluoroborate-based ILs is time-consuming and thus expensive. For this reason, there are only a few examples of IL-based electrolytes for SIBs formed by BF_4^- anions. One example is that of the $\text{NaBF}_4\text{-[C}_2\text{C}_1\text{im]}\text{[BF}_4]$ IL-based electrolyte employed for studying a NASICON ($\text{Na}_3\text{V}_2(\text{PO}_4)_3$) cathode performance [104]. Discharge capacities for NASICON were shown to be lower than those for carbonate electrolytes in the first cycles. However, the $\text{NaBF}_4\text{-[C}_2\text{C}_1\text{im]}\text{[BF}_4]$ electrolyte demonstrated superior cycling and thermal stability. The electrochemical and physical properties of this electrolyte at different sodium concentrations (0.1–0.75 M) were studied by Wu et al. [105]. The ESW widens (4–4.5 V) as the concentration of NaBF_4 increases. In addition, at a concentration of 0.1 M NaBF_4 , the specific conductivity of the IL-based electrolyte is as high as 9.83 mS cm^{-1} .

Sulfonylamide-Based Electrolytes

$\text{NaTFSI}\text{-}[X^+]\text{[TFSI}^-]$ and $\text{NaFSI}\text{-}[X^+]\text{[FSI}^-]$ are widely used due to their high ionic conductivities and relatively facile synthesis. In addition, TFSI^- and FSI^- anions demonstrate low corrosivity for aluminum current collectors. Fisher et al. [106] carried out the synthesis and detailed physicochemical characterization of TFSI^- - and FSI^- -based ILs at room temperature for their application in SIBs (Figure 8). They observed that ILs containing

FSI^- anions have higher ionic conductivities and lower viscosities than those formed by TFSI^- . However, FSI^- -based ILs exhibit lower thermal stability and are less cost-effective than TFSI^- -based ILs. In addition, ILs containing FSI^- anions are highly unstable against hydrolysis [35]. The influence of the cation nature on the electrochemical and physicochemical properties of these ILs was also studied. The results show that the ILs containing ether functionalized cations have the lowest viscosity and the highest conductivity. Table 3 summarizes the main physicochemical properties (viscosity and ionic conductivity) and thermal stability for sulfonylamide-based ILs as studied by Fischer et al. [106]. Importantly, the absence of acidic protons in the cations was demonstrated to yield chemical stability, even in contact with sodium metal.

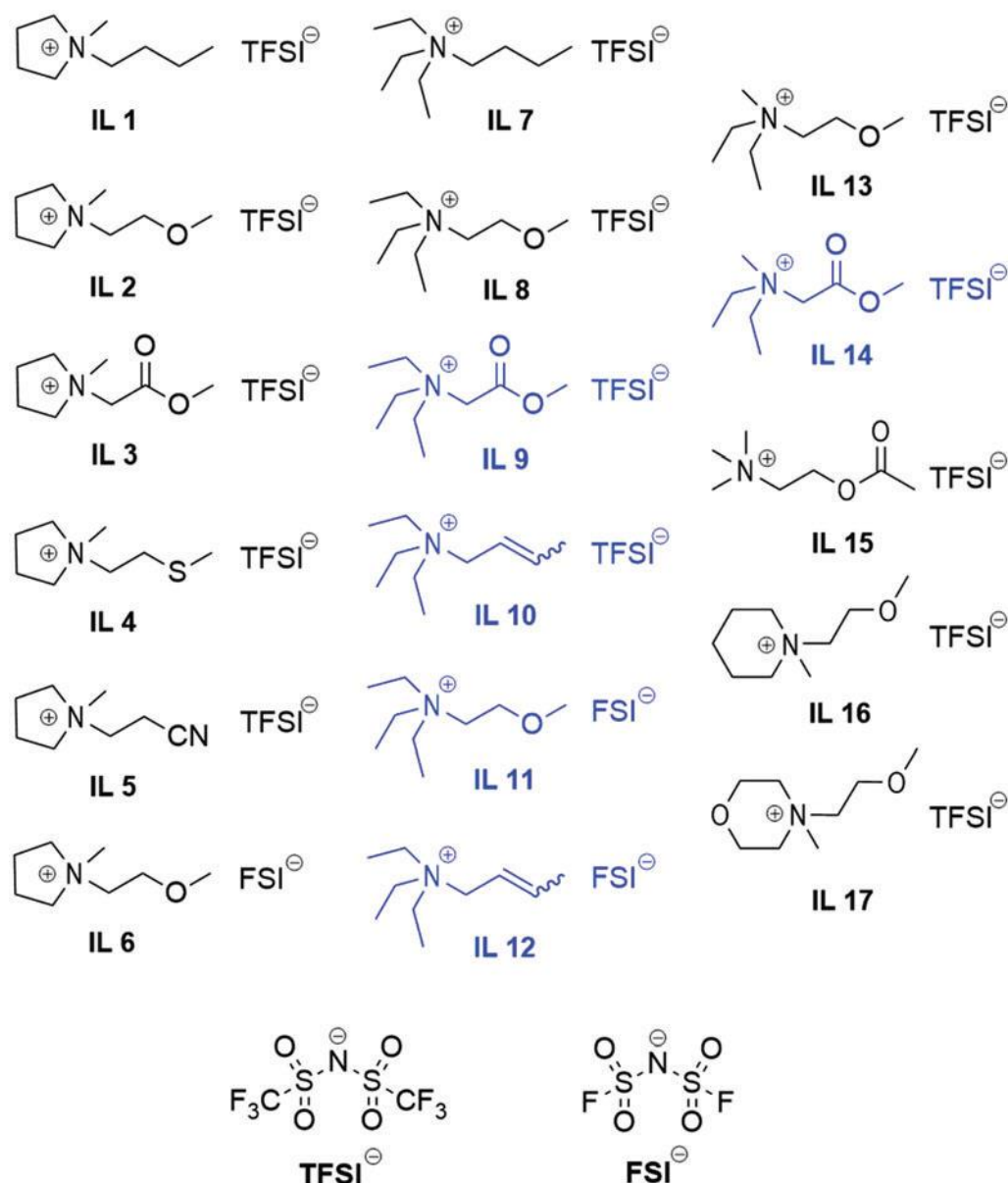


Figure 8. Cations and anions of the ILs studied by Fischer et al. Reproduced with permission [106]. Copyright 2018, Royal Society of Chemistry.

Table 3. Physicochemical properties of ILs with TFSI[−] and FSI[−] anions at room temperature [106].

| Cation | Anion | η (cP) | σ (mS cm ^{−1}) | ESW (V) | Td (°C) | Ref |
|--|-------|-------------|---------------------------------|---------|---------|-------|
| (1-n-butyl-2,3-dimethylimidazolium) (BMMI) | TFSI | 93 | 1.6 | 4.3 | 430 | [107] |
| IL1 | TFSI | 83.5 | 3.26 | 5.14 | 427.5 | |
| IL2/6 | TFSI | 63.0 | 5.26 | 4.98 | 408.6 | |
| IL3 | FSI | 43.6 | 7.66 | 4.89 | 271.2 | |
| IL4 | TFSI | 287.1 | 1.27 | 5.04 | 351.9 | |
| IL5 | TFSI | 222.4 | 1.68 | 3.95 | 286.0 | |
| IL7 | TFSI | 533.8 | 1.28 | 4.91 | 163.4 | |
| IL8/IL11 | TFSI | 156.0 | 1.94 | 5.3 | 396.2 | |
| | | 98.2 | 2.92 | 5.08 | 390.3 | |
| | FSI | 71.8 | 5.07 | 5.02 | 280.4 | [106] |
| IL9 | TFSI | 312.2 | 1.02 | 5.03 | 410.8 | |
| IL10 | TFSI | 156.2 | 1.92 | 4.96 | 345.9 | |
| IL12 | FSI | 119.7 | 3.81 | 4.82 | 261.2 | |
| IL13 | TFSI | 80.1 | 3.99 | 4.92 | 406.5 | |
| IL14 | TFSI | 291.5 | 1.20 | 4.96 | 346.1 | |
| IL15 | TFSI | 256.5 | 1.76 | 5.17 | 367.7 | |
| IL16 | TFSI | 123.4 | 2.64 | 4.96 | 403.7 | |
| IL17 | TFSI | 375.8 | 1.01 | 4.96 | 395.1 | |

Hosokaba et al. [108] studied the stability and the electrochemical performance of $[C_2C_1im]^+$ cation-based IL electrolytes at room temperature. The results show that the electrolyte comprising FSI[−] anions, NaFSI-[C_2C_1im][FSI], is more stable against reduction than the TFSI[−]-based electrolyte, NaTFSI-[C_2C_1im][TFSI]. In addition, NaFSI-[C_2C_1im][FSI] enables sodium plating, in contrast with the case of the NaTFSI-[C_2C_1im][TFSI] electrolyte. Sodium deposition/stripping was also observed to take place at room temperature on a Ni microelectrode in 0.1 M NaTFSI-[C_4C_1pyrr][TFSI], 0.1 NaTFSI-[$N_{2,1,1,3}$][TFSI], and 0.1 M NaTFSI-[$N_{6,2,2,2}$][TFSI] IL-based electrolytes. In 0.1 M NaTFSI-[C_4C_1pyrr][TFSI], the Coulombic efficiency (CE) was reported to be 75% [109], although in general, their values at room temperature were low, with a tendency to rise as temperature increases. In contrast, Wu et al. observed that the CE for Na deposition/stripping using NaFSI-[C_2C_1im][FSI] as an electrolyte was 98.1% at 90 °C after 250 cycles [110]. On the other hand, the deposition/stripping of Na on Ni and Cu collectors was carried out in a NaFSI-[C_3C_1pyrr][FSI] electrolyte at 80 °C (Figure 9a) [111]. The CE value for the sodium deposition/dissolution on Cu was shown to be higher than on Ni. In any case, super-concentrated IL-based electrolytes seem to generate a beneficial SEI layer on the Na metal electrode [112]. The effect of water addition on the SEI formation on Na metal was studied in a super-concentrated NaFSI-[C_3C_1pyrr][FSI] electrolyte. It was demonstrated that the SEI formation is strongly influenced by water addition, which results in distinct chemical composition and morphology. Interestingly, cycling stability was enhanced in Na cells with a water concentration of ~1000 ppm [113,114].

Phosphonium-based ILs have also been shown to be compatible with Na metal. The electrolyte 45 mol% NaFSI-[$P_{1i4i4i4}$][FSI] displayed a CE of 93% in the first cycle and 53% at cycle 20 at 50 mV s^{−1} and at 50 °C. Higher and lower concentrations of the sodium salt led to the formation of a solid phase [112].

Some carbonaceous materials have also been studied as anodes for SIBs using FSI[−] and TFSI[−] one-anion-type IL-based electrolytes. Hard carbon (HC) materials are the most widespread anodes for SIBs. Sun et al. [115] synthesized two HCs with different annealing temperatures (800 and 1300 °C) to study their performance in 3.8 M NaFSI-[C_3C_1pyrr][FSI] IL-based electrolytes. The HC prepared at 1300 °C (100%) showed higher capacity retention after 120 cycles than that prepared at 800 °C (92%) after 114 cycles at 50 mA g^{−1}. In addition,

the hard carbon synthesized at 1300 °C exhibited a specific capacity of 191 mAh g⁻¹ upon 120 cycles. The authors claimed that the differences in the electrochemical performance of the two HCs were due to the formation of SEIs of different nature. Another example is the study of a mesoporous carbon anode (CMK) using either super-concentrated NaFSI-[C₃C₁pyrr][FSI] or an organic electrolyte (1.0 M NaFSI-EC/DMC), both at 50 °C. The SEI formed on the CMK electrode in the IL-based electrolyte is mainly composed of inorganic species (NaF, Na₂O, and sodium sulfides) derived from the FSI⁻ anion decomposition. The SEI outer layer comprises [C₃C₁pyrr]⁺ cations from the IL. For the organic electrolyte, a thick organic-rich SEI layer is generated on the CMK electrode surface (Figure 9b). The Na/CMK cell exhibits a cycle life for the 3.8 M NaFSI-[C₃C₁pyrr][FSI] electrolyte longer than for the organic electrolyte. The capacity value for CMK in IL-based electrolytes after 3500 cycles at 0.5 A g⁻¹ was shown to be as high as 320 mAh g⁻¹ (Figure 9c) [116].

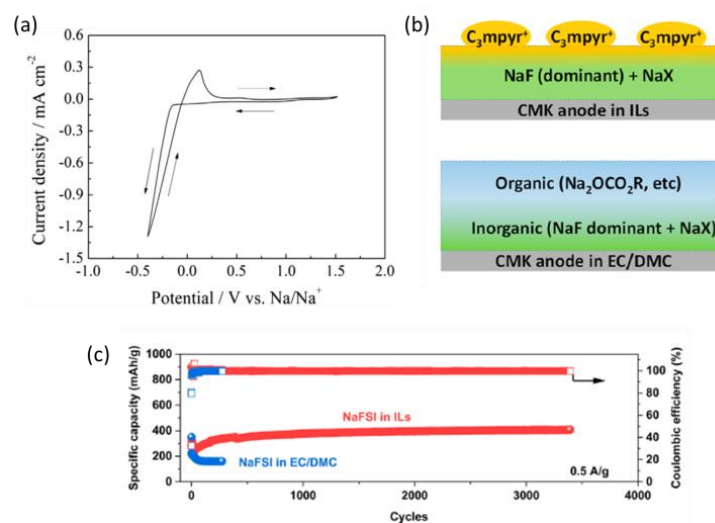


Figure 9. (a) Deposition/stripping of Na on a Ni substrate in NaFSI-[C₃C₁pyrr][FSI] at 80 °C. Reproduced with permission [111]. Copyright 2013, Elsevier. (b) Simplified SEI structure and composition on CMK anodes in contact with either IL-based or carbonate electrolytes where X can be O, S, NSO₂F, SO₃, or CO₃. (c) Measurement for cycling stability of Na/CMK cells in NaFSI-[C₃C₁pyrr][FSI] and carbonate electrolytes at 0.1 A g⁻¹ for the initial 10 cycles and at 0.5 A g⁻¹ for subsequent cycles. Reproduced with permission [116]. Copyright 2021, American Chemical Society.

One-anion-type IL-based electrolytes have been employed for studying the behavior of several SIB cathode materials such as polyanionic compounds (NaFePO₄ [117], Na₂FeP₂O₇ [118], Na₃V₂(PO₄)₃ [119], etc.) and layered transition metal oxides (Na_{2/3}Fe_{1/3}Mn_{2/3}O₂ [120], Na_{2/3}Mn_{0.8}Fe_{0.1}Ti_{0.1}O₂ [100], Na_{0.45}Ni_{0.22}Co_{0.11}Mn_{0.66}O₂ [121], etc.). Organic compounds (calix[4]quinone and 5,7,12,14-pentacenetrone [122]) have also been explored in this context. In general, the cycling stability and reversibility of the different cathode materials are better than in organic electrolytes, particularly for super-concentrated IL-based electrolytes. These improvements are attributed to the high transport number of Na⁺ in super-concentrated electrolytes [100]. Forsyth et al. determined the transport number of Na⁺ in NaFSI-[C₃C₁pyrr][FSI] at different sodium concentrations, with 0.3 for a 50 mol% NaFSI [123]. This result is equivalent to the Li⁺ transport number obtained in a LiPF₆-EC:EMC:DEC (1:1:1) electrolyte, and it agrees with the results reported by Matsumoto et al. [124].

Some examples of the improvement in capacity retention for cathode materials in IL-based electrolytes compared with common organic electrolytes under ambient conditions are described in the following. The P2-type layered oxide Na_{0.84}Li_{0.1}Ni_{0.27}Mn_{0.63}O₂ has been tested in different electrolytes: NaFSI-[C₁C₂im][FSI], NaFSI-[C₄C₁pyrr][FSI]

and NaFSI-[N₁₁₁₄][FSI]. A comparison between the ILs and the NaClO₄-PC electrolyte shows that the capacity exhibited is slightly higher in the organic electrolyte than in the IL-based electrolytes. However, the capacity retention and the cycling stability obtained is better for the IL-based electrolytes (Figure 10a–d) [125]. Another example is the performance study of P2-Na_{0.6}Co_{0.1}Mn_{0.9}O_{2+z} in [C₄C₁pyrr][TFSI] containing different sodium salts (NaTFSI, NaFSI, and NaClO₄) by Do et al. [126], showing results comparable with those for a typical organic electrolyte (NaClO₄-EC/PC). When the one-anion electrolyte NaTFSI-[C₄C₁pyrr][TFSI] is used, the capacity retention improves over that of the organic electrolyte.

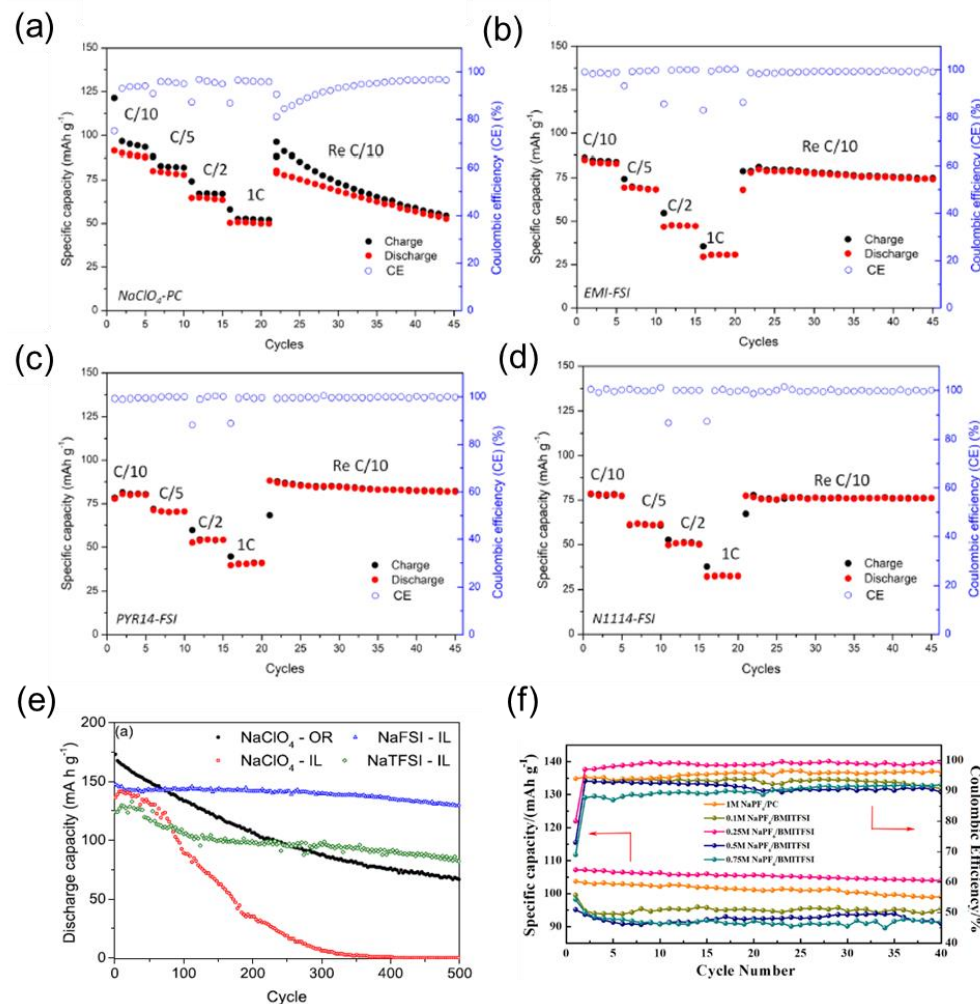


Figure 10. C-rate performance for a Na_{0.84}Li_{0.1}Ni_{0.27}Mn_{0.63}O₂ cathode in different electrolytes under ambient conditions: (a) NaClO₄-PC; (b) NaFSI-[C₁C₂im][FSI]; (c) NaFSI-[C₄C₁pyrr][FSI]; (d) NaFSI-[N₁₁₁₄][FSI] [125]; (e) cycling performance of P2-Na_{0.6}Co_{0.1}Mn_{0.9}O_{2+z} in different electrolytes at 50 mA g⁻¹. Reproduced with permission [126]. Copyright 2019, American Chemical Society; (f) cycling performance and CEs of Na₃V₂(PO₄)₃ for different NaPF₆ concentrations in [C₄C₁im][TFSI] and for a 1.0 M NaPF₆-PC organic electrolyte. Reproduced with permission [127]. Copyright 2018, Elsevier.

2.3.2. Two-Anion-Type Electrolytes

Two-anion-type electrolytes appear as a competitive alternative to one-anion-type electrolytes for improving ion transport and interfacial properties. These advantages would come from changes in the interactions between cations and anions when a second anion is introduced in the electrolyte. In this respect, it has been shown that two-anion-type electrolytes show very low tendency to crystallize, which represents a great advantage

for below-room-temperature applications [128]. On the other hand, it has been observed that using $[N_{2(20201)}_3][TFSI]$ as an IL and using NaFSI instead of NaTFSI as the sodium salt, results in an electrolyte with higher ionic conductivity and lower viscosity at 60 °C for 1.0 and 2.0 M sodium concentrations. These improved physicochemical properties using NaFSI as a sodium salt seem to be due to relatively weak interactions between FSI^- and Na^+ [129]. Similarly, Raman spectroscopy measurements have revealed that the addition of $[NaMM26py]$ to $[C_4C_1PyrTFSI]$ increases the density of free FSI^- anions, improving the conductivity when compared with one-anion-type ILs [130].

Maresca et al. [131] showed reversible sodium insertion/extraction for an HC anode using 0.1NaTFSI-0.9 $[C_2C_1im][FSI]$ and 0.1NaTFSI-0.9 $[N_{1114}][FSI]$ electrolytes at 20 °C. The HC exhibits an initial capacity of 175 mAh g⁻¹ with a capacity retention of 98% after 1500 cycles in 0.1NaTFSI-0.9 $[N_{1114}][FSI]$. The SEI layer formed on the HC in contact with 0.1NaTFSI-0.9 $[C_2C_1im][FSI]$ and 0.1NaTFSI-0.9 $[N_{1114}][FSI]$ is thinner, and it has a higher inorganic content than that formed in the presence of carbonates [131].

Considering again the study of $P2-Na_{0.6}Co_{0.1}Mn_{0.9}O_{2+z}$ by Do et al. [126], the best performance was not obtained for the $TSFI^-$ one-anion-type electrolyte but for the NaFSI- $[C_4C_1pyrr][TFSI]$ two-anion-type electrolyte, with an initial capacity of 147 mAh g⁻¹ and a capacity retention value of 90% after 500 cycles at 50 mA g⁻¹ (Figure 10e). The improvement in performance in the mixed-anion electrolyte was related to the formation of a thinner conductive CEI and a more favorable SEI on the Na metal anode in comparison with the organic electrolyte. Similarly, Chagas et al. [132] demonstrated excellent electrochemical performance for an $Na_{0.45}Ni_{0.22}Co_{0.11}Mn_{0.66}O_2/Na$ cell using a 10 mol% NaTFSI $[C_4C_1pyr][FSI]$ electrolyte. The cell delivered approximately 200 mAh g⁻¹ with an average voltage of 2.7 V, resulting in a specific energy density of 550 Wh kg⁻¹ [132].

The effect of two-anion electrolytes on cathode materials has also been illustrated for $Na/Na_3V_2(PO_4)_3$ cells at room temperature by Wu et al. [127] using $NaPF_6-[C_4C_1im][TFSI]$ as an electrolyte. $Na_3V_2(PO_4)_3$ exhibits capacity values with 0.25 M $NaPF_6-[C_4C_1im][TFSI]$ higher than with 1.0 M $NaPF_6-PC$ (Figure 10f). The ionic conductivity and the EWS measured for this IL-based electrolyte are 3.46 mS cm⁻¹ and 4.6 V, respectively. By means of XPS, FTIR, and EDS analysis, the authors described the formation of a CEI on $Na_3V_2(PO_4)_3$ composed of NaOH, Na_2SO_4 , $Na_2S_2O_7$, and NaF [127].

The search for non-fluorinated electrolytes (anions) has been intensifying in recent years with the purpose of making battery production more environmentally friendly and more cost-effective. In this respect, an interesting candidate is the dicyanamide anion. However, Forsyth et al. [133] showed that an electrolyte formed only by dicyanamide anions, $NaDCA-[C_3C_1pyrr][DCA]$, exhibits limited cycle stability for the sodium deposition/stripping process. These authors also studied the influence of different salt anions on the SEI formation on sodium metal by using the $[C_3C_1pyrr][DCA]$ ionic liquid as a solvent and different Na salts such as NaFSI, NaTFSI, and NaFTFSI. The results show that the electrolyte with the FSI^- anion forms a more stable and thinner SEI layer in comparison with the other two, composed mainly of NaF [133]. Basile et al. also studied the deposition/stripping of Na using an electrolyte based on sodium dicyanamide, $NaDCA-[C_4C_1pyrr][DCA]$, showing that the sodium process is possible when the water content is maintained at 90 ppm [134]. Wongittharom et al. [117] tested the performance of a $NaFePO_4$ cathode material in $[C_4C_1pyrr][TFSI]$ containing different sodium salts ($NaBF_4$, $NaClO_4$, $NaPF_6$, and $NaDCA$) at different temperatures (25, 50, and 75 °C). The $NaBF_4-[C_4C_1pyrr][TFSI]$ electrolyte was shown to exhibit the highest ionic conductivity and the lowest viscosity. The conductivity values at 25 and 75 °C are 1.9 and 4.8 mS cm⁻¹, respectively. However, capacity retention and capacity values exhibited by $NaFePO_4$ are higher in the organic electrolyte. Along the same lines, but using $Na_{0.44}MnO_2$ as a cathode material,

Wang et al. [65] observed that, for a BMP-TFSI-based electrolyte, the use of NaClO_4 seems to be more beneficial for the charge transfer reaction than the use of NaTFSI, leading to better charge–discharge properties. The cell shows an optimum discharge capacity of 97 mAh g^{-1} (at 0.05 C) at 25°C .

In this section, we have described the performance of common ILs in SIBs. ILs were first and more extensively applied to LIBs, from which the main advances were extrapolated to SIBs thanks to the similarities of lithium and sodium. Figure 11 shows the number of publications that have appeared on IL-based electrolytes applied to LIBs and SIBs.

As we mentioned above, the main drawbacks of using ILs as electrolytes are their relatively high cost and their viscosities higher than those of common organic electrolytes. Moreover, ILs sometimes require special handling since they may be contaminated with impurities coming from the synthesis. Despite these disadvantages, they have significant advantages coming from their low volatility and low flammability. In addition, cathode capacities and capacity retention tend to be higher than for typical organic electrolytes. The ESW widths also compare favorably with those for organic electrolytes.

ILs also show promise as additives for organic electrolytes. Organic solvents exhibit low viscosity, high stability, and form electrolytes with relatively good ionic conductivity, while ionic liquids stand out for their thermal and cycling stability. Therefore, by optimizing the ratios of both components it is possible to combine their benefits, with high cost-effectiveness, thus making possible large-scale applications [133,135–139]. Recently, Arkhiova and co-workers observed that adding an organic solvent, such as acetonitrile, can enhance ion solvation in ferrocene-based (Fc) ionic liquids. This, in turn, would facilitate more efficient charge transport, thereby improving overall conductivity [140].

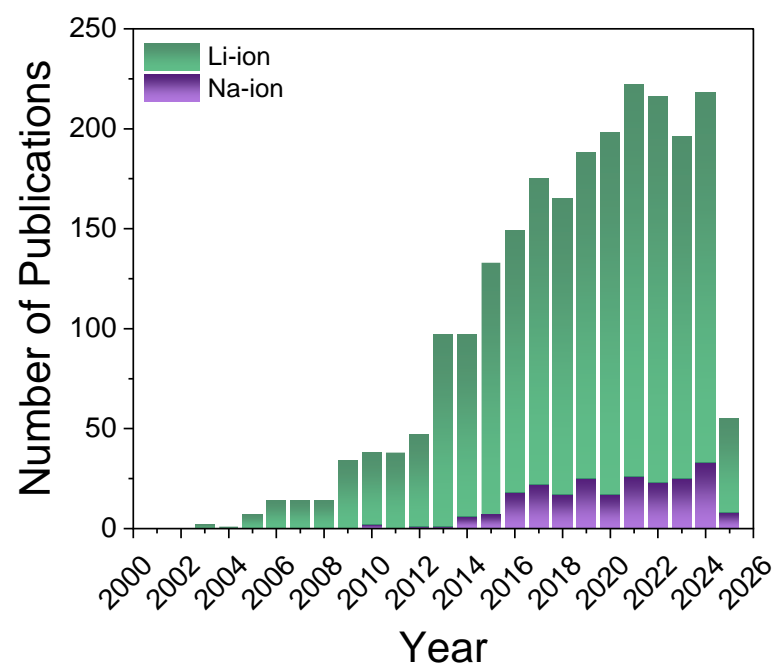


Figure 11. Number of publications per year since 2000 on the use of ILs in lithium and sodium batteries (Scopus, February 2025).

A more cost-effective alternative to the common ILs could be the so-called liquid ammonium electrolytes, which can be considered as quasi-ionic liquids based on their composition and properties. In the following section, we expose the properties and the electrochemical performance of different ammoniums used in the energy storage field.

3. Ammoniates

Ammoniates are simply ammonia solvates of inorganic or hybrid salts. These compounds can be either liquid or solid under ambient conditions. Their formula can be written as $\text{MY}\cdot x\text{NH}_3$, where MY corresponds to the salt (M for the cation and Y for the anion) and x indicates the molar ratio of solvating ammonia to salt. The ammoniates, either liquid or solid, are formed when the corresponding salts absorb anhydrous ammonia, which is a solvating agent characterized by a high dipole moment and the ability to form hydrogen bonds.

As for solid ammoniates, for instance, Zhang et al. synthesized a lithium borohydride ammoniate ($\text{Li}(\text{NH}_3)_n\text{BH}_4$ ($0 < n \leq 2$)) at room temperature via the absorption of ammonia by LiBH_4 [141]. Using the same method, Yan and co-workers prepared $\text{LiBH}_4\cdot\text{NH}_3$ by the exposure of LiBH_4 to dry ammonia gas at a pressure of 1 bar for 2 h at -10°C . For the preparation of $\text{LiBH}_4 \cdot \frac{1}{2}\text{NH}_3$, mechanical milling of $\text{LiBH}_4\cdot\text{NH}_3$ and LiBH_4 in a 1:1 molar ratio was applied [142]. Following a different procedure, Kraus and co-workers left BeF_2 in a reaction vessel with liquid ammonia for four weeks at -40°C . After this period, they reported the formation of colorless crystals on the walls of the vessel ascribed to the beryllium fluoride diammoniate ($\text{BeF}_2(\text{NH}_3)_2$) [143].

On the other hand, liquid ammoniates can be synthesized according to the procedure described by Herlem and co-workers [144]. Prior to the synthesis, all the glassware is cleaned and dried. The dried salt is placed in a reaction flask. An inert atmosphere is created, and the reaction flask is immersed in an acetone solution, which is cooled down to -60°C . Next, an excess of anhydrous ammonia is condensed until the salt is fully dissolved, resulting in a colorless solution. The purification step is carried out by adding an alkali metal to the solution in excess, which triggers the appearance of the blue coloration characteristic of solvated electron solutions (Figure 12a). Solvated electrons are strong reducing agents, reacting with impurities such as H_2O and O_2 . Finally, the solution (colorless) is left to slowly reach room temperature (Figure 12b).

3.1. Properties of Ammoniates

Physical Properties

The ammoniates as electrolytes present remarkable physical characteristics when compared with common organic electrolytes (Table 4). One of the main advantages is their conductivity. In 1988, Badoz-Lambling and co-workers reported a conductivity of 140 mS cm^{-1} at 20°C for $\text{NaI}\cdot 3.3\text{NH}_3$ [145]. Many years later, in 2006, Gonçalves et al. confirmed a conductivity higher than 100 mS cm^{-1} for this sodium iodide ammoniate at 20°C [144]. Recently, Ruiz-Martínez and co-workers [146] measured the specific conductivity of different sodium-based ammoniates used in SIBs. The specific conductivity at 10°C was found to follow the trend $\text{NaBH}_4\cdot 1.5\text{NH}_3 > \text{NaBF}_4\cdot 2.5\text{NH}_3 > \text{NaI}\cdot 3.3\text{NH}_3$, with values of 105, 70, and 60 mS cm^{-1} , respectively. They measured the salt concentration, obtaining values of 7 M, 9 M, and 12 M for $\text{NaI}\cdot 3.3\text{NH}_3$, $\text{NaBF}_4\cdot 2.5\text{NH}_3$, and $\text{NaBH}_4\cdot 1.5\text{NH}_3$, respectively. Ammoniates have a very high ion density, like typical ionic liquids, with the added advantage of having relatively low viscosities and densities [146]. The main difference with typical ionic liquids would be that, for ammoniates, the salt being liquid under ambient conditions is a solvate.

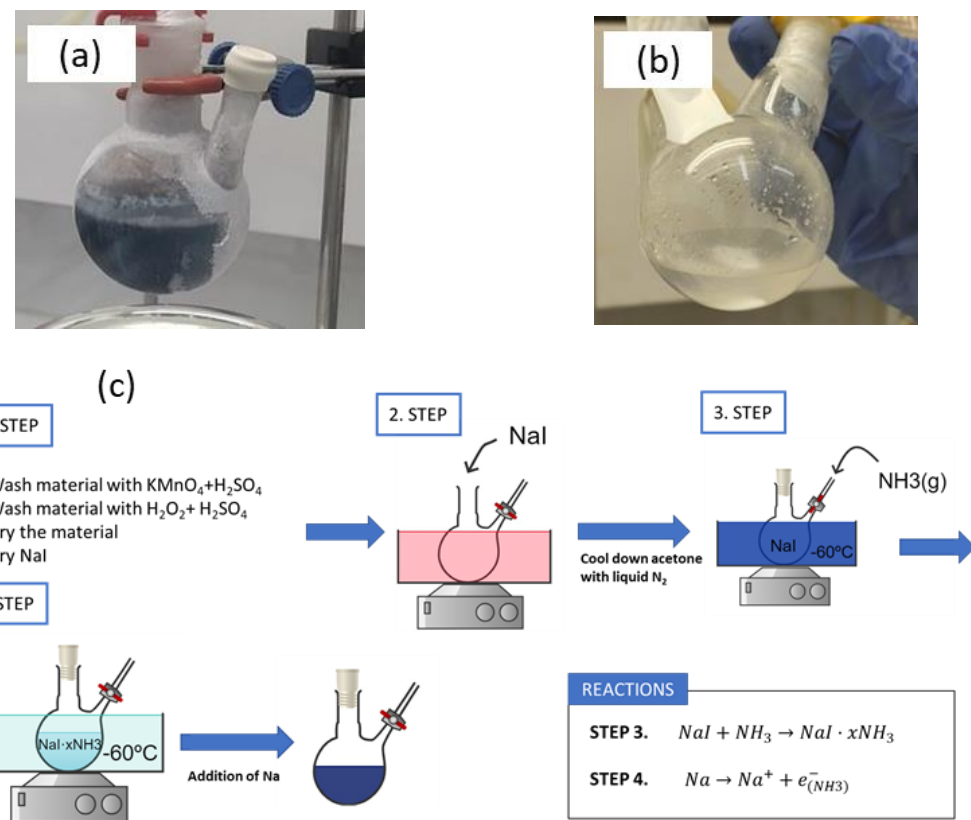


Figure 12. (a) Picture of a sodium salt dissolved in an excess of liquid ammonia containing solvated electrons. (b) Sodium-based liquid ammoniate. (c) Schematic illustration of the synthesis of the sodium iodide liquid ammoniate.

Table 4. Concentration, viscosity, conductivity, and boiling temperature values for common sodium-based organic electrolytes (PC) and sodium-based ammoniates.

| Electrolyte | [C]/M | η/cP | $\sigma/mS\ cm^{-1}$ | Boiling Point */°C | Ref. |
|------------------------|-------|-----------------|----------------------|--------------------|-------|
| $NaClO_4/PC$ | 1 | - | 4.4 | 242 | [146] |
| $NaFSI/DME$ | 3 | - | 9.6 | 80 | [146] |
| $NaPF_6/PC$ | 1 | 9 | 5 | 242 | [147] |
| $NaTFSI/PC$ | 1 | 8 | 5 | 242 | [147] |
| $NaPF_6/PC$ | 3 | 100 | 2 | 242 | [147] |
| $NaTFSI/PC$ | 3 | 90 | 1.5 | 242 | [147] |
| $NaI \cdot 3.3NH_3$ | 7.6 | 9.04 ± 0.02 | 50 | 40 | [146] |
| $NaBF_4 \cdot 1.5NH_3$ | 8.7 | 5.06 ± 0.03 | 70 | 10 | [146] |
| $NaBH_4 \cdot 2.5NH_3$ | 12.3 | 5.54 ± 0.05 | 110 | 18 | [146] |

* For organic solution, the boiling point reported is that of the pure solvent.

Importantly, in the context of their application for batteries, using a highly concentrated electrolyte avoids dendritic growth because there are no transport limitations compared with the typical organic solvents. In fact, the organic electrolytes are usually in the concentration range of 1 M [88,148,149], which enhances a non-uniform ion flux, leading to dendritic growth and to serious safety risks [150].

Organic electrolyte-based metal-ion batteries suffer from another major shortcoming: battery fires and/or explosions, mainly caused by thermal ignition of the carbonate-based electrolyte [151–153]. In this context, ammoniate electrolytes stand out positively since they are non-flammable liquids [146] owing to the intrinsic non-flammable properties of NH_3 . In addition, their high ionic concentration enables a unique solvation structure where most of

the solvent molecules form solvation structures with the cation (Figure 13). As a result, the density of free solvent molecules decreases, significantly suppressing interfacial reactions between the solvent and the electrodes and lowering the battery's flammability [154–156].

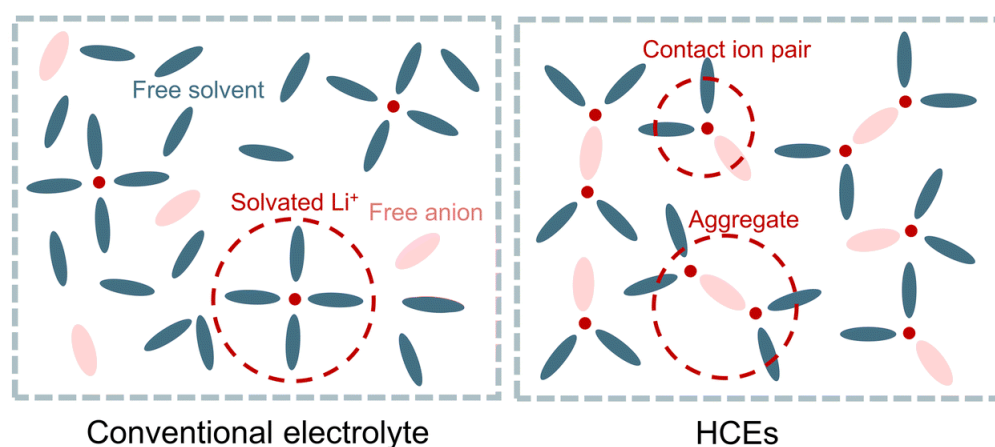


Figure 13. Simple representation of solution structures for conventional and highly concentrated electrolytes (HCEs) Reproduced with permission [155]. Copyright 2023, Royal Society of Chemistry.

As mentioned above, liquid ammoniates potentially have a range of advantages over organic electrolytes. However, these quasi-ionic liquids are very volatile, which restricts their practical application in new rechargeable sodium batteries. In any case, several researchers have reported the use of ammoniates in different fields (see Table 5).

In 2001, Herlem and co-workers described different ammoniates such as $\text{LiNO}_3 \cdot 2\text{NH}_3$, $\text{LiSO}_3\text{CF}_3 \cdot 2\text{NH}_3$, and $\text{Cu}(\text{SO}_3\text{CF}_3)_2$ for electrochromic devices [157]. On the other hand, Yan et al. have reviewed the use of ammoniates for thermal energy storage [158]. In the context of this contribution, it is worth noting that Fujiwara et al. already proposed the use of the NaI liquid ammoniate for thermal energy storage as early as in 1981 [159].

Hydrogen storage constitutes another potential application field for ammoniates. In fact, due to its high specific energy, hydrogen has gained significant attention as a promising energy carrier. However, its low energy density represents a formidable challenge for efficient and safe storage. Owing to their hydrogen storage capacities, metal hydrides (MgH_2 , LiH) [160], metal alanates (MAIH_4 ; $\text{M} = \text{Li, Na, Mg, Ca}$) [161,162], metal borohydrides (MBH_4 ; $\text{M} = \text{Li, Na, Ca, Mg, Zn}$) [163–165], and ammonia-based compounds such as H_3NBH_3 [166] are potential alternatives. Among them, metal borohydrides require high operation temperatures (higher than 400°C) since their thermal decomposition is a highly endothermic process ($\sim 67 \text{ kJ/mol H}_2$, for LIBH_4 partial decomposition to LiH , B , and H_2) [167,168]. Interestingly, metal borohydride properties can be improved by complexing them with ammonia, forming metal borohydride ammoniates ($\text{MBH}_4 \cdot x\text{NH}_3$). Some reported examples are $\text{LiBH}_4 \cdot \text{NH}_3$ [169], $\text{Mg}(\text{BH}_4)_2 \cdot 6\text{NH}_3$ [170], $\text{Ca}(\text{BH}_4)_2 \cdot 2\text{NH}_3$ [171], and $\text{Al}(\text{BH}_4)_2 \cdot 6\text{NH}_3$ [172]. These ammoniates release hydrogen in the temperature range of 150 – 400°C [173]. Several researchers have claimed that the decomposition temperature of metal borohydrides decreases with increasing electronegativity of metal cations [174]. In this regard, bimetallic borohydride ammoniates such as $\text{Li}_2\text{Al}(\text{BH}_4)_5 \cdot 6\text{NH}_3$ and $\text{NaZn}(\text{BH}_4)_3 \cdot 2\text{NH}_3$ have been reported in the literature [175,176].

Table 5. Summary of different applications for ammoniates.

| Application field | Ammoniate | State | Ref. |
|------------------------|---|--------|-------------------|
| Electrochromic devices | NH ₄ NO ₃ ·1.5NH ₃ | Liquid | [177] |
| | LiNO ₃ ·2NH ₃ | Liquid | [157] |
| | LiSO ₃ CF ₃ ·2NH ₃ | Liquid | [157] |
| | Cu (SO ₃ CF ₃) ₂ | Liquid | [157] |
| | NaSO ₃ CF ₃ ·2.9NH ₃ | Liquid | [157] |
| Thermal storage | NH ₄ SCN·xNH ₃ | Liquid | [159] |
| | NiCl ₂ ·xNH ₃ | Solid | [158] |
| | BaCl ₂ ·xNH ₃ | Solid | [158] |
| | CoCl ₂ ·xNH ₃ | Solid | [158] |
| | MnCl ₂ ·xNH ₃ | Solid | [158] |
| | SrCl ₂ ·xNH ₃ | Solid | [158] |
| | CaCl ₂ ·xNH ₃ | Solid | [158] |
| | NaBr·xNH ₃ | Solid | [158] |
| Hydrogen storage | Mg(BH ₄) ₂ ·6NH ₃ | Solid | [170] |
| | LiBH ₄ ·NH ₃ | Solid | [169] |
| | Ca(BH ₄) ₂ ·2NH ₃ | Solid | [171] |
| | Al(BH ₄) ₂ ·6NH ₃ | Solid | [172] |
| | Li ₂ Al(BH ₄) ₅ ·6NH ₃ | Solid | [175] |
| | NaZn(BH ₄) ₃ ·2NH ₃ | Solid | [176] |
| Batteries | LiClO ₄ ·4NH ₃ | Liquid | [145] |
| | NaI·3.3NH ₃ | Liquid | [145,146,178–180] |
| | LiNO ₃ ·xNH ₃ | Liquid | [181] |
| | LiSO ₃ CF ₃ ·xNH ₃ | Liquid | [181] |
| | NaBF ₄ ·2.5NH ₃ , | Liquid | [146] |
| | NaBH ₄ ·1.5NH ₃ | Liquid | [146] |
| | Li(NH ₃) _n BH ₄ | Solid | [141] |
| | LiTFSI·xNH ₃ | Liquid | [182] |
| | BeF ₂ (NH ₃) ₂ | Solid | [143] |

3.2. Ammoniates for Batteries

Herlem and co-workers were the first to use ammoniates as electrolytes for primary batteries in 1988 [145]. They initially reported on the use of LiClO₄·4NH₃ and NaI·3.3NH₃. Later in 1991, they studied LiNO₃·xNH₃ ($1.5 < x < 3.1$) and LiSO₃CF₃·xNH₃ ($1.5 < x < 3.5$) in the same context [181]. These ammoniates show high specific conductivity, around $0.1 \Omega^{-1} \text{ cm}^{-1}$, with ESWs of 3.9 V (vs. Li⁺/Li) for that of LiSO₃CF₃ and 3.5 V (vs. Li⁺/Li) for that of LiNO₃.

In 2006, Gonçalves et al. [144] proposed the sodium iodide ammoniate as an electrolyte for redox batteries, achieving a cell voltage of 2 V. It was the first time that an alkali metal deposition/stripping was reported to exhibit fully reversible redox behavior, except for molten salts [144]. Since then, a few researchers have reported on the use of ammoniates as SIB electrolytes. Ruiz-Martinez et al. [146] did extensive research on these electrolytes and their application in SIBs. In 2017 [146], they studied the plating/stripping of sodium using three different sodium-based ammoniates (NaBF₄·2.5NH₃, NaBH₄·1.5NH₃, and NaI·3.3NH₃). Figure 14a,b show cyclic voltammograms (CVs) for a symmetric sodium cell with two different organic electrolytes: (a) 3 M NaFSI/DME and (b) 1 M NaClO₄/PC. As observed, the current density decreases with the cycles. They attributed this decay to reactions occurring between the organic electrolyte and the sodium metal surface. Unlike organic electrolytes, sodium-based ammoniates (Figure 14c) show stable sodium plating/stripping. Despite applying overpotentials limited to $\pm 100 \text{ mV}$ (vs. Na⁺/Na), lower than those used for organic electrolytes, significantly higher current density values were recorded. This

indicates that the kinetics of Na plating/stripping is faster in sodium-based ammoniates than in typical organic electrolytes.

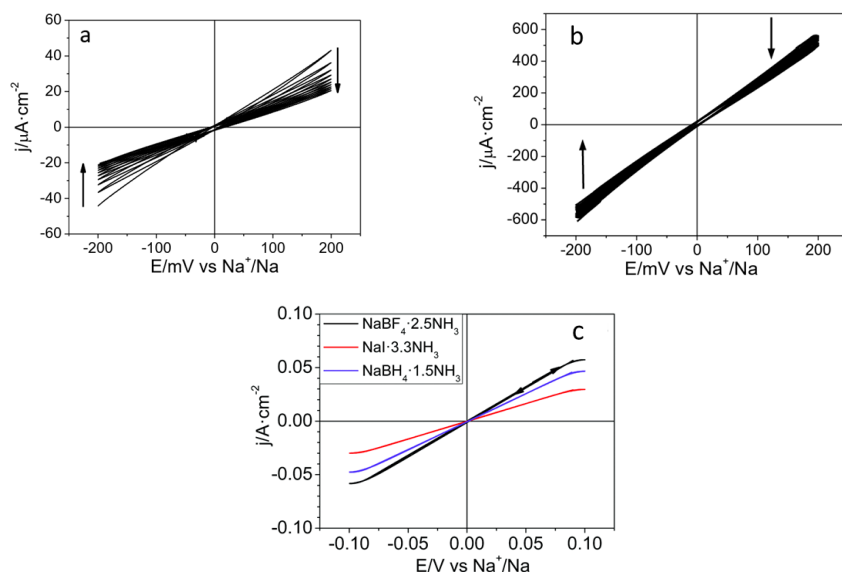


Figure 14. CVs for the sodium plating/stripping process in a symmetric $\text{Na}/\text{NaI}\cdot3.3\text{NH}_3$ cell at a scan rate of 20 mV s^{-1} in the range of $\pm 0.2 \text{ V}$ vs. Na^+/Na in (a) 3 M NaFSI/DME and (b) 1 M NaClO_4/PC . (c) CVs for Na deposition/stripping over Na (supported on Cu) at a scan rate of 10 mV s^{-1} in three ammoniates. Reproduced with permission [146]. Copyright 2017, Royal Society of Chemistry.

Excess amounts of sodium decrease the actual specific and volumetric capacity of battery cells [183,184]. In this context, anode-less batteries (ALB) have attracted growing attention in recent years, and they are considered a potentially promising configuration for next-generation energy storage systems [185–187]. Ruiz-Martínez et al. [146] studied the sodium deposition/dissolution process on Al/C and Cu substrates using the sodium-based ammoniates mentioned above. The results demonstrate quasi-stationary voltammetric behavior for Cu, with virtually 100% CE (Figure 15).

To gain further insights by simulating a first charge process in an ALB, a chronoamperometry experiment was carried out by applying a potential of -100 mV vs. Na^+/Na for 100 s. Subsequently, the cell was cycled from 100 to 600 times at a current density of 0.01 A cm^{-2} (Figure 16). The resulting voltage hysteresis ranges from 5 mV to 10 mV for $\text{NaBF}_4\cdot2.5\text{NH}_3$ and $\text{NaBH}_4\cdot1.5\text{NH}_3$, respectively, while for $\text{NaI}\cdot3.3\text{NH}_3$, it reaches a value of 18 mV. These low hysteresis values disclose rapid kinetics for sodium plating and stripping, enabling good cyclability.

The performance of electrodes composed of amorphous TiO_2 nanotubes was also studied by Ruiz-Martínez and Gómez using $\text{NaI}\cdot3.3\text{NH}_3$ and 1M NaClO_4/PC as electrolytes in sodium half cells [178]. The liquid ammoniate leads to significantly larger specific capacities (between 0.5 and 2.6 V vs. Na^+/Na): $145 \text{ mAh g}^{-1}_{\text{TiO}_2}$ in $\text{NaI}\cdot3.3\text{NH}_3$ vs. $105 \text{ mAh g}^{-1}_{\text{TiO}_2}$ in 1M NaClO_4/PC at 1 mA cm^{-2} . However, at 0.1 mA cm^{-2} , the capacity values were closer ($160 \text{ mAh g}^{-1}_{\text{TiO}_2}$ in 1 M NaClO_4/PC vs. $175 \text{ mAh g}^{-1}_{\text{TiO}_2}$ in $\text{NaI}\cdot3.3\text{NH}_3$). As shown in Figure 17, the ammoniate shows at high C rates (14 C, 1 mA) a superior performance since it does not suffer from significant transport limitations thanks to its very high values of sodium concentration and specific conductivity.

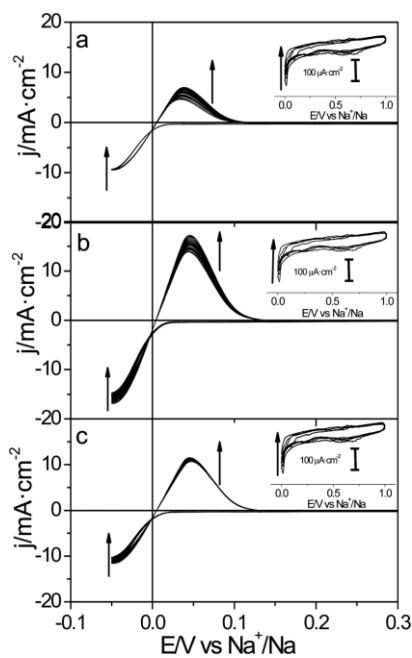


Figure 15. Cyclic voltammograms for the Na^+/Na process on Cu substrates at 20 mV s^{-1} using as electrolytes (a) $\text{NaI} \cdot 3.3\text{NH}_3$, (b) $\text{NaBH}_4 \cdot 1.5\text{NH}_3$, and (c) $\text{NaBF}_4 \cdot 2.5\text{NH}_3$. Reproduced with permission [146]. Copyright 2017, Royal Society of Chemistry.

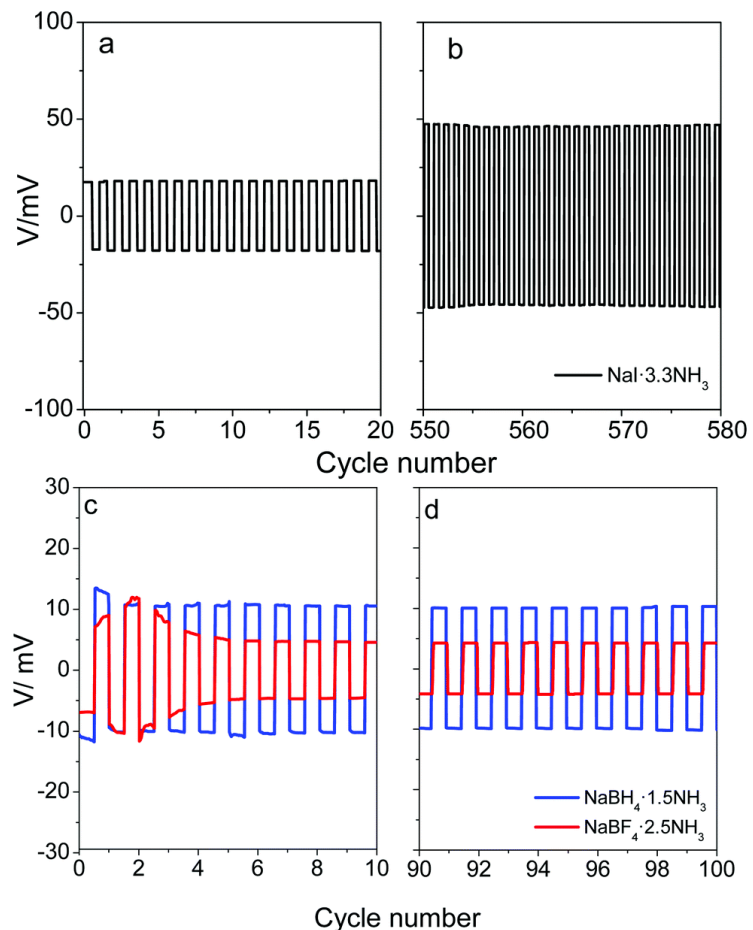


Figure 16. Charge–discharge curves for Na plating/stripping on a Cu collector at a current density of 10 mA cm^{-2} in $\text{NaI} \cdot 3.3\text{NH}_3$ (a,b), and in $\text{NaBH}_4 \cdot 1.5\text{NH}_3$ and $\text{NaBF}_4 \cdot 2.5\text{NH}_3$ electrolytes (c,d). Reproduced with permission [146]. Copyright 2017, Royal Society of Chemistry.

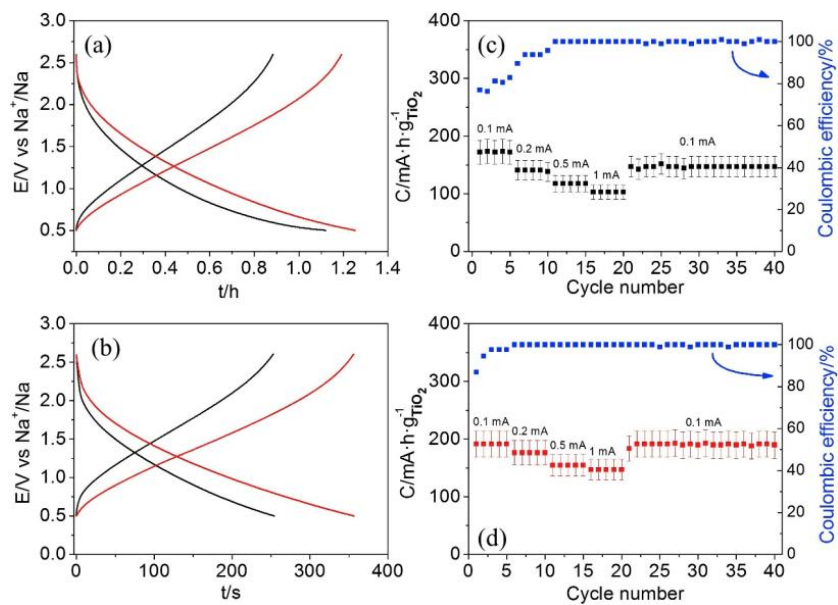


Figure 17. Charge/discharge curves for TiO₂ nanotube (NT) electrodes at (a) 0.1 mA cm⁻² or (b) 1 mA cm⁻² in either NaI·3.3NH₃ (red line) or 1 M NaClO₄/PC (black line). Coulombic efficiency and specific capacity as a function of the number of cycles for TiO₂ NT electrodes at different C rates for (c) 1 M NaClO₄ in PC and (d) NaI·3.3NH₃. Reproduced with permission [178]. Copyright, 2019 Elsevier.

On the other hand, the use of organic cathodes such as indanthrone blue (IB) in ammonium-based batteries has recently been reported. The IB molecule possesses four carbonyl groups, and it can thus exchange up to four electrons in its redox processes, achieving a theoretical capacity of 242 mAh g⁻¹. The battery provides excellent rate performance with a specific capacity of at least 120 mAh g⁻¹_{IB} at 10 C (1.2 A g⁻¹_{IB}) over 1000 cycles and a specific power above 2 kW kg⁻¹_{IB} at 20 °C (Figure 18) [179]. Experiments were also carried out with the IB electrode in NaBF₄·2.5NH₃. This ammonium is interesting as NaBF₄ is significantly more cost-effective than NaI, and additionally, it can lead to systems with ESWs wider than NaI [146]. It shows an initial discharge capacity of 163 mAh g⁻¹_{IB}, and after 5 cycles, it reaches a maximum value of 188 mAh g⁻¹_{IB}, maintaining it for around 90 cycles. These values are higher than those achieved using NaI·3.3NH₃ because the sodium tetrafluoroborate ammonium has a higher conductivity and sodium concentration as well as a wider ESW (by 0.3 V) than the NaI ammoniate at 4 °C [146]. However, during battery operation in the tested ammoniates, the IB becomes partially dissolved in the electrolyte and typically suffers from volume changes or an irreversible phase transformation, which results in limited cyclability and rapid capacity decay [188].

To mitigate the issues found with the IB dye, strategies such as polymerization or immobilization of the organic molecule on stable conductive carbon matrices have been proposed [189,190]. In this context, a cost-effective SIB using poly(anthraquinonyl sulfide) (PAQS) as a cathode material and sodium metal as an anode has been proposed and tested. This configuration exhibits a discharge capacity of 218 mAh g⁻¹ at 5 C with a CE of almost 100% over 300 cycles. The Na/NaI·3.3NH₃/PAQS battery system showed a superior rate performance (~200 mAh g⁻¹ even at 62 C or 10,400 mA g⁻¹_{PAQS}) and exhibited an average specific energy density of 324 Wh kg⁻¹_{PAQS} and a high-power density of 3500 W kg⁻¹_{PAQS} at 20 °C over 100 cycles. These interesting results come from the very low charge transfer resistance in the ammoniates. Moreover, this battery system, with a mass loading of 8 mg cm⁻², has a capacity retention of 80% over 150 cycles at 5C without

any major capacity loss [180]. These values are significantly higher than those reported for analogous systems based on organic electrolytes using comparable C rates [191,192].

Recently, the use of a new hybrid conjugated microporous polymer (CMP) containing anthraquinone redox moieties has been proposed as a cathode material for ammoniate-based batteries (IEP-11-SR) [193]. This polymer enables the preparation of a self-standing cathode, which coupled with $\text{NaI}\cdot 3.3\text{NH}_3$ as an electrolyte, yielded an extraordinary kinetic performance and high Na^+ diffusion coefficient ($D_{\text{Na}^+} = 2\cdot 10^{-7} \text{ cm}^2\text{s}^{-1}$). Regarding electrochemical performance, the system exhibited high capacity (100 mAh g⁻¹ at 1C (0.3 mA cm⁻²)) and excellent rate capability, retaining 52% of its capacity at 250 C (52 mAh g⁻¹ at 95 mA cm⁻²). Moreover, solubility issues were overcome, achieving 4000 charge–discharge cycles at 15 C (4.5 mA cm⁻²), with a capacity retention exceeding 70% (59 mAh g⁻¹) (Figure 19).

Despite the wide range of advantages and great performance of ammoniates demonstrated in recent years (see Table 6), their development and application for SIBs are still hampered by their high volatility and relatively poor electrochemical stability. The ESW widths for $\text{NaBH}_4\cdot 1.5\text{NH}_3$, $\text{NaBF}_4\cdot 2.5\text{NH}_3$, and $\text{NaI}\cdot 3.3\text{NH}_3$ are 3.1, 3.3, and 2.8 V, respectively [146]. These values, compared with those of typical organic electrolytes and ILs are quite low, which could be a limitation in the utilization of the ammoniates as electrolytes. In fact, low attainable voltages not only affect specific energy and power values but they also reduce the range of potential cathode materials, excluding those with higher redox potentials. Improving these properties would enable designing a sustainable, safe, highly conducting, and cost-effective room-temperature electrolyte for secondary batteries.

Another interesting approach would be to develop solid ammoniates, which are likely to improve the thermal and electrochemical stability of the electrolyte. One increasingly important example is that of the previously mentioned borohydride-based ammoniates. To the best of our knowledge, only a few researchers have recently reported on their use in magnesium- and lithium-based rechargeable batteries (see Table 6), making further investigation in this topic highly valuable [141,194–200].

Table 6. Energy density, cycle performance, and working voltages for batteries based on different magnesium-, lithium-, and sodium-based ammoniates.

| Ammoniate | Cathode/Anode | Capacity/mAh g ⁻¹ | Specific Energy/ Wh kg ⁻¹ | Cyclability | Working Voltages/V | Ref |
|---|-----------------------|------------------------------|---|-----------------|--------------------------------|-------|
| $\text{LiClO}_4\cdot 4\text{NH}_3$ (liq.) | (SN) _x /Li | | 300 | | | |
| | MnO_2 /Li | - | 320 | - | From OCP (2.8, 3 and 2.6) to 1 | [145] |
| | CuO /Li | | 92 | | | |
| $\text{LiNO}_3\cdot x\text{NH}_3$ (liq.) | MnO_2 /Li | - | ≈650 | - | From OCP (3.5) to 2 | [181] |
| $\text{LiSO}_3\text{CF}_3\cdot x\text{NH}_3$ (liq.) | MnO_2 /Li | - | ≈650 | - | From OCP (3.9) to 2 | [181] |
| $\text{LiTFSI}\cdot x\text{NH}_3$ (liq.) | MnO_2 /Li | - | ≈600 | - | - | [182] |
| $\text{NaBF}_4\cdot 2.5\text{NH}_3$ (liq.) | IB/Na | 188 | 275 | 90 at 8C (4 °C) | 3–1.2 | [179] |
| $\text{NaI}\cdot 3.3\text{NH}_3$ (liq.) | (SN) _x /Li | | 190 | | | |
| | MnO_2 /Li | - | 213 | - | - | [145] |
| | CuO /Li | | 72 | | | |
| | TiO_2 /Na | 145 | 73 | 400 at 14C | 2.6–0.5 | [178] |
| | IB/Na | ≈100 | 210 | 1000 at 10C | 2.5–1.3 | [179] |
| $\text{Li}(\text{NH}_3)_{0.5}\text{BH}_4@\text{SiO}_2$ (s.) | PAQS/Na | 218 | 320 (after 100 cycles) | 300 at 11C | 2.6–1.2 | [180] |
| | (IEP-11-SR)/Na | 100 at 1C | - | 4000 at 15C | 2.5–1.1 | [193] |
| | SPAN/Li | 800 at 0.2C | - | <10 | 0–2.4 V | [197] |
| Mg(BH ₄) ₂ ·2NH ₃ (s.) | TiS ₂ /Mg | 141 (1st cycle) at 0.05C | - | 30 | 0–1.4 V | [198] |

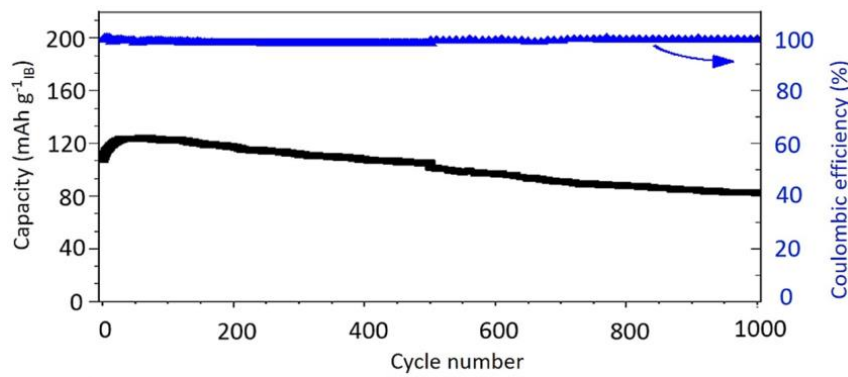


Figure 18. Specific capacity vs. number of cycles for an IB electrode in $\text{NaI}\cdot 3.3\text{NH}_3$ at 10 C. Reproduced with permission [179]. Copyright, 2023 Elsevier.

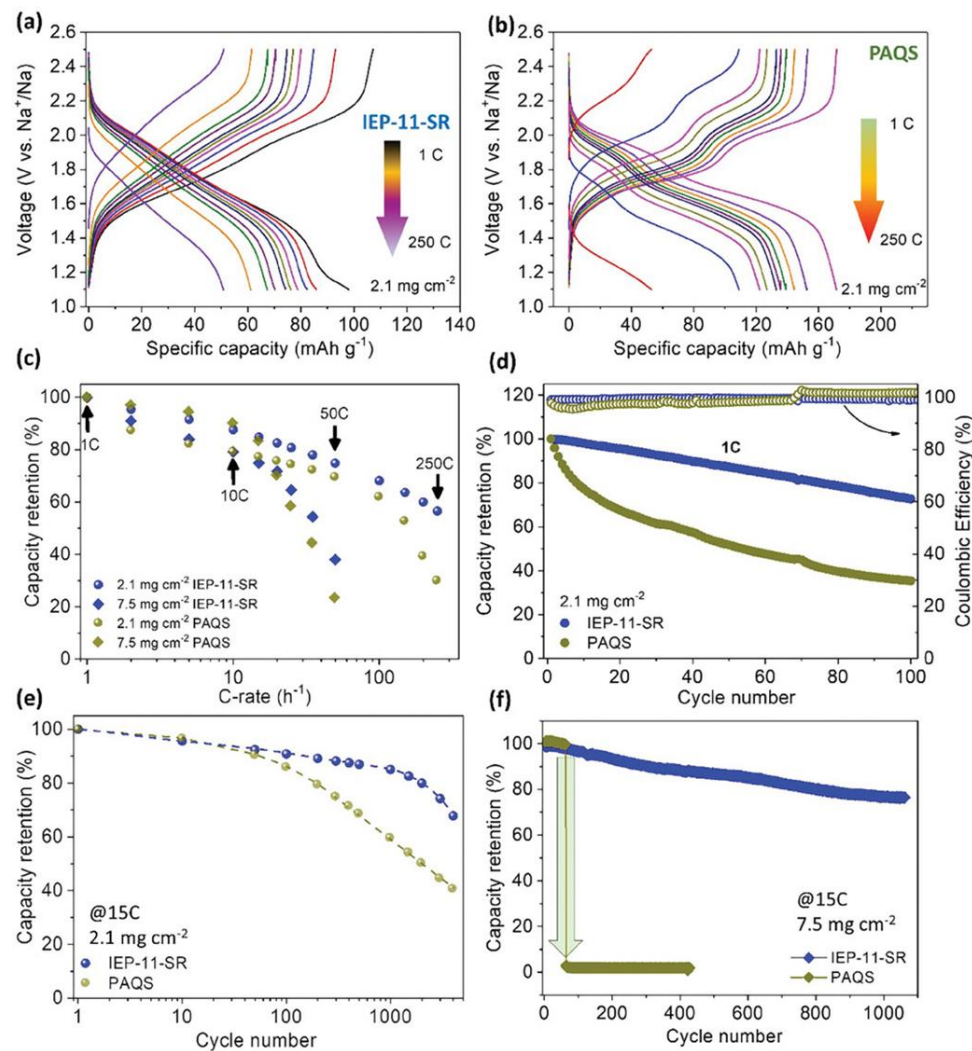


Figure 19. Charge-discharge curves for a sodium metal battery (SMB) at different C rates with 2.1 mg cm^{-2} mass loading using as cathodes: (a) IEP-11-SR (conjugated microporous polymer) and (b) PAQS. (c) Capacity retentions of SMBs vs. C rate with either IEP-11-SR or PAQS cathodes with mass loadings of 2.1 and 7.5 mg cm^{-2} . (d) Cyclability experiments of SMBs at 1C with either IEP-11-SR or PAQS cathodes and using mass loading of 2.1 mg cm^{-2} . Capacity retention of SMBs vs. number of cycles at 15C for either IEP-11-SR or PAQS cathodes and mass loadings of (e) 2.1 mg cm^{-2} and (f) 7.5 mg cm^{-2} . Reproduced with permission [193]. Copyright, 2024 Wiley.

4. Summary and Perspective

In recent years, the so-called “beyond Li-ion” battery technologies have garnered significant interest. With growing concerns about LIBs’ environmental and economic impacts, SIBs have emerged as a promising alternative. In fact, sodium is one of the most attractive choices for the development of large-scale energy storage applications due to its abundance and cost-effectiveness. Since sodium is more readily available than lithium, production costs as well as environmental effects can be minimized. Additionally, sodium-based batteries can be transported at zero voltage, unlike lithium batteries, which require a minimum charge for storage. This makes them safer devices overall. To achieve high-performance SIBs, it is essential to develop advanced electrode materials that enable high electrochemical performance. Likewise, the electrolyte is also a central component for the development of advanced SIB technologies. An ideal electrolyte should have a wide electrochemical window, high thermal stability, and exceptional ionic conductivity to achieve superior performance. In the current state of the art, most electrolytes for SIBs are made of organic salts dissolved in carbonate and ether solvents. However, they suffer from low thermal stability and relatively poor electrochemical performance because of the formation of non-uniform and fragile SEIs.

In this review, we have dwelled on the use of ILs as alternative electrolytes for SIBs, with a focus on the less explored family of quasi-ILs known as liquid ammoniates. We have classified ILs into protic and aprotic, the latter being those most frequently used in SIBs. The nature of the ILs gives them unique properties such as high ionic conductivity, excellent thermal, chemical and electrochemical stability, negligible vapor pressure, and high miscibility with other compounds. However, their synthesis is a time-consuming and costly process.

Although ILs have appealing properties that make them potential alternatives to organic electrolytes, their high cost is undoubtedly a significant barrier for most applications. Their expensive synthesis and the requirement of high purity have hindered the scale-up of SIBs using IL-based electrolytes. To overcome these challenges, different synthetic methods applying electrodialysis, ultrasound, and microwaves are being explored to both increase environmental friendliness and reduce overall cost. Another approach that would reduce the final cost is to use ILs as additives in organic electrolytes.

On the other hand, we consider ammoniates to be a promising family of electrolytes for SIBs since they share with ILs some of their most attractive properties, but with the added advantage of high ionic conductivities with extremely high sodium concentrations, relatively low viscosities and densities, and high cost-effectiveness (Figure 20). In this contribution, we have highlighted these excellent physicochemical properties and ensuing advantages together with their potential use in other applications. It is worth noting once again that sodium plating and stripping processes are extremely reversible in liquid ammoniates, with CEs being virtually equal to 100%, not only for sodium metal but also for current collectors of other materials such as copper. This enables their application in the development of anode-free batteries. The use of ammoniate-based electrolytes avoids the formation of SEIs on sodium metal surfaces, which, together with high sodium concentrations, leads to uniform and dendrite-free sodium deposition.

Admittedly, the prospects of using ILs as electrolytes in the future battery landscape will depend on the reduction in their cost and viscosity. In the case of liquid ammoniates, the main drawbacks are thermodynamic instability in contact with sodium, a relatively narrow electrochemical stability window, and high volatility. Currently, as far as we know, there are no publications unveiling and demonstrating strategies for overcoming these issues in the case sodium-based batteries. Work needs to be completed in this respect to enhance the applicability of these electrolytes. We believe that a thorough exploration of

solid ammoniates may be a plausible way to advance, which would also be aligned with current tendencies in battery development.

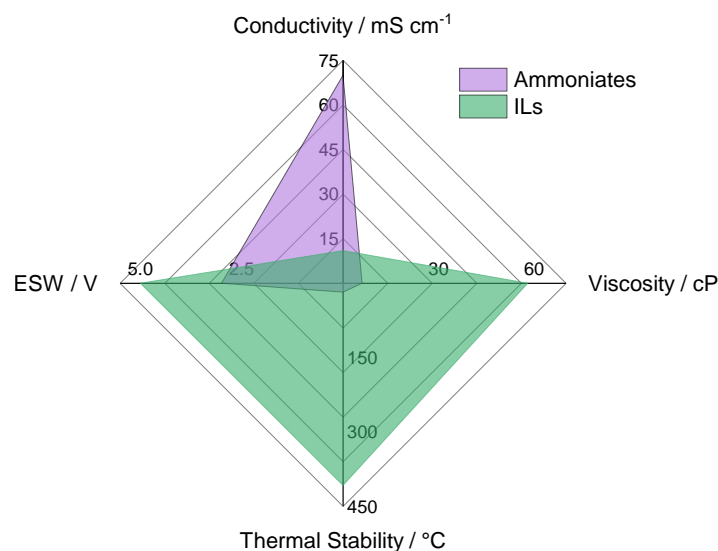


Figure 20. Average values of some key properties of sodium-based ammoniates and ILs. Data taken from Tables 2 and 4.

Author Contributions: P.H.-V. Visualization, writing—original draft preparation. C.M. Visualization, writing—original draft preparation. A.P.-P. writing—original draft preparation, and supervision. R.G. Supervision, writing—review and editing, and funding acquisition. All authors have read and agreed to the published version of the manuscript.

Funding: This research was funded by MCIN/AEI/10.13039/501100011033 and the European Union “NextGenerationEU”/PRTR through project PLEC2021-007779 entitled “Innovative electrolytes and electrodes for a new generation of sodium batteries for stationary applications (NABASTAT)”.

Acknowledgments: A.P.-P. is grateful to the Ministry of Universities, the European Union “NextGenerationEU” and the University of Alicante for the award of a María Zambrano Fellowship.

Conflicts of Interest: The authors declare no conflicts of interest.

Abbreviations

| Abbreviation | Ionic liquid |
|-----------------------|---|
| MEIC | 1-methyl-3-ethylimidazolium chloride |
| CnC1pyrr+ | N-alkyl-N-methylpyrrolidinium |
| CnC1im+ | N-alkyl-N-methylimidazolium |
| CnC1pip+ | N-alkyl-N-methylpiperidinium |
| Nnnnn+ | Tetraalkylammonium |
| AS(m,n)+ | Azoniastri[<i>m,n</i>]nonane |
| Pnnnn+ | Tetraalkylphosphonium. |
| BF4– | Tetrafluoroborate |
| PF6– | Hexafluorophosphate |
| N(CN)2– | Dicyanamide |
| TFSI– | Bis(trifluoromethanesulfonyl)imide |
| FSI– | Bis(fluorosulfonyl)imide |
| [C4Hpyrr][TFSI] | N-butylpyrrolidinium-bis(trifluoromethanesulfonyl)imide |
| LiTFSI | Lithium bis(trifluoromethanesulfonyl)imide |
| NaTFSI [C4Pyrr][TFSI] | Sodium bis(trifluoromethanesulfonyl)imide N-butylpyrrolidinium-Bis(trifluoromethanesulfonyl)imide |

| | |
|---------------------|---|
| NaBF4 | Sodium tetrafluoroborate |
| NaPF6 | Sodium hexafluorophosphate |
| NaClO4 | Sodium perchlorate |
| NaTFSI | Sodium bis(trifluoromethanesulfonyl)imide |
| NaFSI [C2C1im][FSI] | Sodium bis(fluoromethanesulfonyl)imide [1-ethyl-3methylimidazolium] [bis(fluorosulfonyl)imide] |
| [C2C1im][BF4] | 1-ethyl-3-methylimidazolium tetrafluoroborate |
| [C4C1im][OTf] | 1-butyl-3-methylimidazolium trifluoromethanesulfonate |
| [CnC1im]+ | N-alkyl-N-methylimidazolium |
| [CnC1im][TFSI] | N-alkyl-N-methylimidazolium bis(trifluoromethylsulfonyl)imide |
| [CnC1pyrr][TFSI] | N-alkyl-N-methylpyrrolidinium bis(trifluoromethylsulfonyl)imide |
| [CnCnpip][TFSI] | N-alkyl-N-alkylpiperidinium bis(trifluoromethanesulfonyl)imide |
| [C4C1im][TFSI] | 1-butyl-3-methylimidazolium bis(trifluoromethanesulfonyl)imide |
| [C4C1im][FSI] | 1-butyl-3-methylimidazolium bis(fluorosulfonyl)imide |
| [C4C1im][BF4] | 1-butyl-3-methylimidazolium tetrafluoroborate |
| [C4C1im][PF6] | 1-butyl-3-methylimidazolium hexafluorophosphate |
| [C4C1im][DCA] | 1-butyl-3-methylimidazolium dicyanamide |
| [C2C1im][TFSI] | 1-ethyl, 3-methylimidazolium bis(trifluoromethanesulfonyl)imide |
| [C2C1im][FSI] | 1-ethyl, 3-methylimidazolium bis(fluorosulfonyl)imide |
| [C2C1im][DCA] | 1-ethyl, 3-methylimidazolium dicyanamide |
| [C2C1im][OTf] | 1-ethyl, 3-methylimidazolium trifluoromethanesulfonate |
| [C4C1pyrr][TFSI] | N-butyl-N-methylpyrrolidinium bis(trifluoromethylsulfonyl)imide |
| [C4C1pyrr][FSI] | N-butyl-N-methylpyrrolidinium bis(fluorosulfonyl)imide |
| [C4C1pyrr][DCA] | N-butyl-N-methylpyrrolidinium Dicyanamide |
| [C3C1pyrr][TFSI] | N-propyl-N-methylpyrrolidinium bis(trifluoromethylsulfonyl)imide |
| [C3C1pyrr][FSI] | N-propyl-N-methylpyrrolidinium bis(fluorosulfonyl)imide |
| [N2,1,1,3][TFSI] | N-ethyldimethylpropylammonium bis(trifluoromethylsulfonyl)imide |
| [N2,2,2,5][TFSI] | Triethylpentylammonium bis(trifluoromethylsulfonyl)imide |
| [N4441][FSI] | Tributylmethylammonium bis(fluorosulfonyl)imide |
| [N1114][TFSI] | Butyltrimethylammonium bis(trifluoromethylsulfonyl)imide |
| [C2C1im][BF4] | 1-ethyl, 3-methylimidazolium tetrafluoroborate |
| [C4C1pyrr][TFSI] | N-butyl-N-methylpyrrolidinium bis(trifluoromethylsulfonyl)imide |
| [C3C1pyrr][DCA] | N-methyl,N-propyl pyrrolidinium dicyanamide |
| [N1114][FSI] | N-trimethyl-N-butyl-ammonium bis(fluorosulfonyl)imide |
| [N2,1,1,3][TFSI] | N-ethyldimethylpropylammonium bis(trifluoromethylsulfonyl)imide |
| [N6,2,2,2][TFSI] | N-hexyltriethylammonium bis(trifluoromethylsulfonyl)imide |
| [P1i4i4i4][FSI] | Tri(isobutyl)methylphosphonium bis(fluorosulfonyl)imide |
| NaN(CN)2 | Sodium dicyanamide |
| MM26py | 1-methylpyridinium 2,6-dicarboxylate |

References

- “Data Page: Share of Electricity Generated by Renewables”. Part of the Following Publication: Hannah Ritchie, Pablo Rosado and Max Roser (2023)—“Energy”. *Data adapted from Ember, Energy Institute*. Available online: <https://ourworldindata.org/grapher/share-electricity-renewables> (accessed on 21 October 2024).
- Electricity Generation by Source 2023 | Statista. Available online: <https://www.statista.com/statistics/269811/world-electricity-production-by-energy-source/> (accessed on 21 October 2024).
- El Pacto Verde Europeo—Comisión Europea. Available online: https://commission.europa.eu/strategy-and-policy/priorities-2019-2024/european-green-deal_es (accessed on 21 October 2024).
- REPowerEU. Available online: https://ec.europa.eu/commission/presscorner/detail/en/ip_22_3131 (accessed on 21 October 2024).
- Renewables Take the Lead in Power Generation in 2023—Eurostat. Available online: <https://ec.europa.eu/eurostat/web/products-eurostat-news/w/ddn-20240627-1> (accessed on 21 October 2024).

6. Balali, M.H.; Nouri, N.; Omrani, E.; Nasiri, A.; Otieno, W. An Overview of the Environmental, Economic, and Material Developments of the Solar and Wind Sources Coupled with the Energy Storage Systems. *Int. J. Energy Res.* **2017**, *41*, 1948–1962. [[CrossRef](#)]
7. Mahmoud, M.; Ramadan, M.; Olabi, A.G.; Pullen, K.; Naher, S. A Review of Mechanical Energy Storage Systems Combined with Wind and Solar Applications. *Energy Convers. Manag.* **2020**, *210*, 112670. [[CrossRef](#)]
8. Kebede, A.A.; Kalogiannis, T.; Van Mierlo, J.; Berecibar, M. A Comprehensive Review of Stationary Energy Storage Devices for Large Scale Renewable Energy Sources Grid Integration. *Renew. Sustain. Energy Rev.* **2022**, *159*, 112213. [[CrossRef](#)]
9. Li, C.; Xu, H.; Ni, L.; Qin, B.; Ma, Y.; Jiang, H.; Xu, G.; Zhao, J.; Cui, G. Nonaqueous Liquid Electrolytes for Sodium-Ion Batteries: Fundamentals, Progress and Perspectives. *Adv. Energy Mater.* **2023**, *13*, 2301758. [[CrossRef](#)]
10. CATL Unveils Its Latest Breakthrough Technology by Releasing Its First Generation of Sodium-Ion Batteries. Available online: <https://www.catl.com/en/news/665.html> (accessed on 21 October 2024).
11. Peters, J.F.; Baumann, M.; Binder, J.R.; Weil, M. On the Environmental Competitiveness of Sodium-Ion Batteries under a Full Life Cycle Perspective—A Cell-Chemistry Specific Modelling Approach. *Sustain. Energy Fuels* **2021**, *5*, 6414–6429. [[CrossRef](#)]
12. International Energy Agency. *Global EV Outlook 2023: Catching Up with Climate Ambitions*; International Energy Agency: Paris, France, 2023.
13. Sodium Ion VS LiFePO₄ Battery Compared: Pros, Cons, and Differences—ECO Teardown. Available online: <https://ecoteardown.top/sodium-ion-vs-lifepo4-battery-compared-pros-cons-and-differences/> (accessed on 21 October 2024).
14. Sodium-Ion vs. Lithium-Ion Battery: Comparison, Challenges & Alternative | GEP Blog. Available online: <https://www.gep.com/blog/strategy/lithium-ion-vs-sodium-ion-battery> (accessed on 21 October 2024).
15. Perveen, T.; Siddiq, M.; Shahzad, N.; Ihsan, R.; Ahmad, A.; Shahzad, M.I. Prospects in Anode Materials for Sodium Ion Batteries—A Review. *Renew. Sustain. Energy Rev.* **2020**, *119*, 109549. [[CrossRef](#)]
16. Qiao, S.; Zhou, Q.; Ma, M.; Liu, H.K.; Dou, S.X.; Chong, S. Advanced Anode Materials for Rechargeable Sodium-Ion Batteries. *ACS Nano* **2023**, *17*, 11220–11252. [[CrossRef](#)]
17. Kumar Prajapati, A.; Bhatnagar, A. A Review on Anode Materials for Lithium/Sodium-Ion Batteries. *J. Energy Chem.* **2023**, *83*, 509–540. [[CrossRef](#)]
18. Wang, W.; Li, W.; Wang, S.; Miao, Z.; Liu, H.K.; Chou, S. Structural Design of Anode Materials for Sodium-Ion Batteries. *J. Mater. Chem. A Mater.* **2018**, *6*, 6183–6205. [[CrossRef](#)]
19. Gupta, P.; Pushpakanth, S.; Haider, M.A.; Basu, S. Understanding the Design of Cathode Materials for Na-Ion Batteries. *ACS Omega* **2022**, *7*, 5605–5614. [[CrossRef](#)]
20. Nguyen, T.P.; Kim, I.T. Recent Advances in Sodium-Ion Batteries: Cathode Materials. *Materials* **2023**, *16*, 6869. [[CrossRef](#)] [[PubMed](#)]
21. Zhang, H.; Gao, Y.; Liu, X.; Zhou, L.; Li, J.; Xiao, Y.; Peng, J.; Wang, J.; Chou, S.L. Long-Cycle-Life Cathode Materials for Sodium-Ion Batteries toward Large-Scale Energy Storage Systems. *Adv. Energy Mater.* **2023**, *13*, 2300149. [[CrossRef](#)]
22. Xu, S.; Dong, H.; Yang, D.; Wu, C.; Yao, Y.; Rui, X.; Chou, S.; Yu, Y. Promising Cathode Materials for Sodium-Ion Batteries from Lab to Application. *ACS Cent. Sci.* **2023**, *9*, 2012–2035. [[CrossRef](#)] [[PubMed](#)]
23. Xue, Z.; Zhu, D.; Shan, M.; Wang, H.; Zhang, J.; Cui, G.; Hu, Z.; Gordon, K.C.; Xu, G.; Zhu, M. Functional Separator Materials of Sodium-Ion Batteries: Grand Challenges and Industry Perspectives. *Nano Today* **2024**, *55*, 102175. [[CrossRef](#)]
24. Yi, M.; Jing, M.; Deng, W.; Zou, G.; Hou, H.; Wu, T.; Ji, X. Electrolyte, Separator, Binder and Other Devices of Sodium Ion Batteries. In *Sodium-Ion Batteries: Technologies and Applications*; Wiley: Hoboken, NJ, USA, 2023; pp. 171–245. [[CrossRef](#)]
25. Luo, W.; Cheng, S.; Wu, M.; Zhang, X.; Yang, D.; Rui, X. A Review of Advanced Separators for Rechargeable Batteries. *J. Power Sources* **2021**, *509*, 230372. [[CrossRef](#)]
26. Hashmi, M.M.; Arif, N.A.; Ali, S.M.; Khan, M.B.; Singh, M.P.; Khan, Z.H. Recent Progress in Separators for Rechargeable Batteries. In *Materials Horizons: From Nature to Nanomaterials*; Springer: Singapore, 2022; pp. 417–498. [[CrossRef](#)]
27. Huang, Z.X.; Zhang, X.L.; Zhao, X.X.; Zhao, Y.Y.; Aravindan, V.; Liu, Y.H.; Geng, H.; Wu, X.L. Electrode/Electrolyte Additives for Practical Sodium-Ion Batteries: A Mini Review. *Inorg. Chem. Front.* **2022**, *10*, 37–48. [[CrossRef](#)]
28. Huang, Y.; Zhao, L.; Li, L.; Xie, M.; Wu, F.; Chen, R. Electrolytes and Electrolyte/Electrode Interfaces in Sodium-Ion Batteries: From Scientific Research to Practical Application. *Adv. Mater.* **2019**, *31*, 1808393. [[CrossRef](#)]
29. Usiskin, R.; Lu, Y.; Popovic, J.; Law, M.; Balaya, P.; Hu, Y.S.; Maier, J. Fundamentals, Status and Promise of Sodium-Based Batteries. *Nat. Rev. Mater.* **2021**, *6*, 1020–1035. [[CrossRef](#)]
30. Tian, Z.; Zou, Y.; Liu, G.; Wang, Y.; Yin, J.; Ming, J.; Alshareef, H.N. Electrolyte Solvation Structure Design for Sodium Ion Batteries. *Adv. Sci.* **2022**, *9*, 2201207. [[CrossRef](#)]
31. Gao, X.; Xing, Z.; Wang, M.; Nie, C.; Shang, Z.; Bai, Z.; Dou, S.X.; Wang, N. Comprehensive Insights into Solid-State Electrolytes and Electrode-Electrolyte Interfaces in All-Solid-State Sodium-Ion Batteries. *Energy Storage Mater.* **2023**, *60*, 102821. [[CrossRef](#)]
32. Tawalbeh, M.; Ali, A.; Aljawneh, B.; Al-Othman, A. Progress in Safe Nano-Structured Electrolytes for Sodium Ion Batteries: A Comprehensive Review. *Nano-Struct. Nano-Objects* **2024**, *39*, 101311. [[CrossRef](#)]

33. Ahmad, H.; Kubra, K.T.; Butt, A.; Nisar, U.; Iftikhar, F.J.; Ali, G. Recent Progress, Challenges, and Perspectives in the Development of Solid-State Electrolytes for Sodium Batteries. *J. Power Sources* **2023**, *581*, 233518. [CrossRef]
34. Wang, Y.; Song, S.; Xu, C.; Hu, N.; Molenda, J.; Lu, L. Development of Solid-State Electrolytes for Sodium-Ion Battery—A Short Review. *Nano Mater. Sci.* **2019**, *1*, 91–100. [CrossRef]
35. Domingues, L.S.; de Melo, H.G.; Martins, V.L. Ionic Liquids as Potential Electrolytes for Sodium-Ion Batteries: An Overview. *Phys. Chem. Chem. Phys.* **2023**, *25*, 12650–12667. [CrossRef]
36. Zhou, W.; Zhang, M.; Kong, X.; Huang, W.; Zhang, Q. Recent Advance in Ionic-Liquid-Based Electrolytes for Rechargeable Metal-Ion Batteries. *Adv. Sci.* **2021**, *8*, 2004490. [CrossRef]
37. Xu, C.; Yang, G.; Wu, D.; Yao, M.; Xing, C.; Zhang, J.; Zhang, H.; Li, F.; Feng, Y.; Qi, S.; et al. Roadmap on Ionic Liquid Electrolytes for Energy Storage Devices. *Chem. Asian J.* **2021**, *16*, 549–562. [CrossRef]
38. Walden, P. Molecular Weights and Electrical Conductivity of Several Fused Salts. *Bull. Acad. Imper. Sci.* **1914**, *1800*, 405–422.
39. Welton, T. Ionic Liquids: A Brief History. *Biophys. Rev.* **2018**, *10*, 691–706.
40. Poole, C.F.; Furton, K.G.; Kersten, B.R. Liquid Organic Salt Phases for Gas Chromatography. *J. Chromatogr. Sci.* **1986**, *24*, 400–409.
41. Hussey, C.L. Room Temperature Molten Salt Systems. *Adv. Molten Salt Chem.* **1983**, *5*, 185–230.
42. Pacholec, F.; Butler, H.T.; Poole, C.F. Molten Organic Salt Phase for Gas-Liquid Chromatography. *Anal. Chem.* **1982**, *54*, 1938–1941. [CrossRef]
43. Magnuson, D.K.; Bodley, J.W.; Evans, D.F. The Activity and Stability of Alkaline Phosphatase in Solutions of Water and the Fused Salt Ethylammonium Nitrate. *J. Solut. Chem.* **1984**, *13*, 583–587. [CrossRef]
44. Evans, D.F.; Chen, S.H.; Schriver, G.W.; Arnett, E.M. Thermodynamics of Solution of Nonpolar Gases in a Fused Salt. “Hydrophobic Bonding” Behavior in a Nonaqueous System. *J. Am. Chem. Soc.* **1981**, *103*, 481–482. [CrossRef]
45. Schubert, T.J.S. Current and Future Ionic Liquid Markets. In *Ionic Liquids: Current State and Future Directions*; ACS Symposium Series; American Chemical Society: Washington, DC, USA, 2017; Volume 1250, pp. 35–65, ISBN 9780841232136.
46. Sood, K.; Saini, Y.; Thakur, K.K. Ionic Liquids in Catalysis: A Review. *Mater. Today Proc.* **2023**, *81*, 739–744. [CrossRef]
47. Singh, V.V.; Nigam, A.K.; Batra, A.; Boopathi, M.; Singh, B.; Vijayaraghavan, R. Applications of Ionic Liquids in Electrochemical Sensors and Biosensors. *Int. J. Electrochem.* **2012**, *2012*, 165683. [CrossRef]
48. Jónsson, E. Ionic Liquids as Electrolytes for Energy Storage Applications—A Modelling Perspective. *Energy Storage Mater.* **2020**, *25*, 827–835. [CrossRef]
49. Watanabe, M.; Thomas, M.L.; Zhang, S.; Ueno, K.; Yasuda, T.; Dokko, K. Application of Ionic Liquids to Energy Storage and Conversion Materials and Devices. *Chem. Rev.* **2017**, *117*, 7190–7239. [CrossRef]
50. Lim, J.R.; Chua, L.S.; Mustaffa, A.A. Ionic Liquids as Green Solvent and Their Applications in Bioactive Compounds Extraction from Plants. *Process Biochem.* **2022**, *122*, 292–306. [CrossRef]
51. Gray, G.E.; Kohl, P.A.; Winnick, J. Stability of Sodium Electrodeposited from a Room Temperature Chloroaluminate Molten Salt. *J. Electrochem. Soc.* **1995**, *142*, 3636–3642. [CrossRef]
52. Scordilis-Kelleya, C.; Carlin, R.T. Stability and Electrochemistry of Lithium in Room Temperature Chloroaluminate Molten Salts. *J. Electrochem. Soc.* **1994**, *141*, 873–875. [CrossRef]
53. Eshetu, G.G.; Jeong, S.; Pandard, P.; Lecocq, A.; Marlair, G.; Passerini, S. Comprehensive Insights into the Thermal Stability, Biodegradability, and Combustion Chemistry of Pyrrolidinium-Based Ionic Liquids. *ChemSusChem* **2017**, *10*, 3146–3159. [CrossRef] [PubMed]
54. Matsumoto, K.; Hwang, J.; Kaushik, S.; Chen, C.Y.; Hagiwara, R. Advances in Sodium Secondary Batteries Utilizing Ionic Liquid Electrolytes. *Energy Environ. Sci.* **2019**, *12*, 3247–3287. [CrossRef]
55. Stettner, T.; Balducci, A. Protic Ionic Liquids in Energy Storage Devices: Past, Present and Future Perspective. *Energy Storage Mater.* **2021**, *40*, 402–414. [CrossRef]
56. Brutti, S.; Simonetti, E.; De Francesco, M.; Sarra, A.; Paolone, A.; Palumbo, O.; Fantini, S.; Lin, R.; Falgayrat, A.; Choi, H.; et al. Ionic Liquid Electrolytes for High-Voltage, Lithium-Ion Batteries. *J. Power Sources* **2020**, *479*, 228791. [CrossRef]
57. Gao, X.; Wu, F.; Mariani, A.; Passerini, S. Concentrated Ionic-Liquid-Based Electrolytes for High-Voltage Lithium Batteries with Improved Performance at Room Temperature. *ChemSusChem* **2019**, *12*, 4185–4193. [CrossRef]
58. Freemantle, M. *An Introduction to Ionic Liquids*; Royal Society of Chemistry: London, UK, 2010.
59. Brandt, A.; Pires, J.; Anouti, M.; Balducci, A. An Investigation about the Cycling Stability of Supercapacitors Containing Protic Ionic Liquids as Electrolyte Components. *Electrochim. Acta* **2013**, *108*, 226–231. [CrossRef]
60. Arnaiz, M.; Huang, P.; Ajuria, J.; Rojo, T.; Goikolea, E.; Balducci, A. Protic and Aprotic Ionic Liquids in Combination with Hard Carbon for Lithium-Ion and Sodium-Ion Batteries. *Batter. Supercaps* **2018**, *1*, 204–208. [CrossRef]
61. Menne, S.; Schroeder, M.; Vogl, T.; Balducci, A. Carbonaceous Anodes for Lithium-Ion Batteries in Combination with Protic Ionic Liquids-Based Electrolytes. *J. Power Sources* **2014**, *266*, 208–212. [CrossRef]
62. Lingua, G.; Falco, M.; Stettner, T.; Gerbaldi, C.; Balducci, A. Enabling Safe and Stable Li Metal Batteries with Protic Ionic Liquid Electrolytes and High Voltage Cathodes. *J. Power Sources* **2021**, *481*, 228979. [CrossRef]

63. Vogl, T.; Vaalma, C.; Buchholz, D.; Secchiaroli, M.; Marassi, R.; Passerini, S.; Balducci, A. The Use of Protic Ionic Liquids with Cathodes for Sodium-Ion Batteries. *J. Mater. Chem. A Mater.* **2016**, *4*, 10472–10478. [[CrossRef](#)]
64. Basile, A.; Hilder, M.; Makhlooghiyazad, F.; Pozo-Gonzalo, C.; MacFarlane, D.R.; Howlett, P.C.; Forsyth, M. Ionic Liquids and Organic Ionic Plastic Crystals: Advanced Electrolytes for Safer High Performance Sodium Energy Storage Technologies. *Adv. Energy Mater.* **2018**, *8*, 1703491. [[CrossRef](#)]
65. Wang, C.H.; Yeh, Y.W.; Wongittharom, N.; Wang, Y.C.; Tseng, C.J.; Lee, S.W.; Chang, W.S.; Chang, J.K. Rechargeable Na/Na_{0.44}MnO₂ Cells with Ionic Liquid Electrolytes Containing Various Sodium Solutes. *J. Power Sources* **2015**, *274*, 1016–1023. [[CrossRef](#)]
66. Babuccı, M.; Akçay, A.; Balcı, V.; Uzun, A. Thermal Stability Limits of Imidazolium Ionic Liquids Immobilized on Metal-Oxides. *Langmuir* **2015**, *31*, 9163–9176. [[CrossRef](#)]
67. Cao, Y.; Mu, T. Comprehensive Investigation on the Thermal Stability of 66 Ionic Liquids by Thermogravimetric Analysis. *Ind. Eng. Chem. Res.* **2014**, *53*, 8651–8664. [[CrossRef](#)]
68. Matsumoto, K.; Hosokawa, T.; Nohira, T.; Hagiwara, R.; Fukunaga, A.; Numata, K.; Itani, E.; Sakai, S.; Nitta, K.; Inazawa, S. The Na[FSA]–[C2C1im][FSA] (C2C1im+·1-Ethyl-3-Methylimidazolium and FSA–:Bis(Fluorosulfonyl)Amide) Ionic Liquid Electrolytes for Sodium Secondary Batteries. *J. Power Sources* **2014**, *265*, 36–39. [[CrossRef](#)]
69. Mondal, T.; Samanta, P. Study of Physicochemical Properties of Ionic Liquids. In *Handbook of Ionic Liquids*; John Wiley & Sons, Ltd.: Hoboken, NJ, USA, 2024; pp. 51–67. ISBN 9783527839520.
70. Zhang, S.; Sun, N.; He, X.; Lu, X.; Zhang, X. Physical Properties of Ionic Liquids: Database and Evaluation. *J. Phys. Chem. Ref. Data* **2006**, *35*, 1475–1517.
71. Coadou, E.; Goodrich, P.; Neale, A.R.; Timperman, L.; Hardacre, C.; Jacquemin, J.; Anouti, M. Synthesis and Thermophysical Properties of Ether-Functionalized Sulfonium Ionic Liquids as Potential Electrolytes for Electrochemical Applications. *ChemPhysChem* **2016**, *17*, 3992–4002. [[CrossRef](#)]
72. Zhang, H.; Feng, W.; Nie, J.; Zhou, Z. Recent Progresses on Electrolytes of Fluorosulfonimide Anions for Improving the Performances of Rechargeable Li and Li-Ion Battery. *J. Fluor. Chem.* **2015**, *174*, 49–61. [[CrossRef](#)]
73. Kazemiabnavi, S.; Zhang, Z.; Thornton, K.; Banerjee, S. Electrochemical Stability Window of Imidazolium-Based Ionic Liquids as Electrolytes for Lithium Batteries. *J. Phys. Chem. B* **2016**, *120*, 5691–5702. [[CrossRef](#)]
74. Mousavi, M.P.S.; Wilson, B.E.; Kashefolgheta, S.; Anderson, E.L.; He, S.; Bühlmann, P.; Stein, A. Ionic Liquids as Electrolytes for Electrochemical Double-Layer Capacitors: Structures That Optimize Specific Energy. *ACS Appl. Mater. Interfaces* **2016**, *8*, 3396–3406. [[CrossRef](#)]
75. Fitchett, B.D.; Rollins, J.B.; Conboy, J.C. 1-Alkyl-3-Methylimidazolium Bis(Perfluoroalkylsulfonyl)Imide Water-Immiscible Ionic Liquids. *J. Electrochem. Soc.* **2005**, *152*, E251. [[CrossRef](#)]
76. Appetecchi, G.B.; Montanino, M.; Zane, D.; Carewska, M.; Alessandrini, F.; Passerini, S. Effect of the Alkyl Group on the Synthesis and the Electrochemical Properties of N-Alkyl-N-Methyl-Pyrrolidinium Bis(Trifluoromethanesulfonyl)Imide Ionic Liquids. *Electrochim. Acta* **2009**, *54*, 1325–1332. [[CrossRef](#)]
77. Montanino, M.; Carewska, M.; Alessandrini, F.; Passerini, S.; Appetecchi, G.B. The Role of the Cation Aliphatic Side Chain Length in Piperidinium Bis(Trifluoromethansulfonyl)Imide Ionic Liquids. *Electrochim. Acta* **2011**, *57*, 153–159. [[CrossRef](#)]
78. Hwang, J.; Matsumoto, K.; Hagiwara, R. Electrolytes toward High-Voltage Na₃V₂(PO₄)₂F₃ Positive Electrode Durable against Temperature Variation. *Adv. Energy Mater.* **2020**, *10*, 2001880. [[CrossRef](#)]
79. Rogers, E.I.; Šljukic, B.; Hardacre, C.; Compton, R.G. Electrochemistry in Room-Temperature Ionic Liquids: Potential Windows at Mercury Electrodes. *J. Chem. Eng. Data* **2009**, *54*, 2049–2053. [[CrossRef](#)]
80. Randström, S.; Appetecchi, G.B.; Lagergren, C.; Moreno, A.; Passerini, S. The Influence of Air and Its Components on the Cathodic Stability of N-Butyl-N-Methylpyrrolidinium Bis(Trifluoromethanesulfonyl)Imide. *Electrochim. Acta* **2007**, *53*, 1837–1842. [[CrossRef](#)]
81. Zheng, Y.; Wang, D.; Kaushik, S.; Zhang, S.; Wada, T.; Hwang, J.; Matsumoto, K.; Hagiwara, R. Ionic Liquid Electrolytes for Next-Generation Electrochemical Energy Devices. *EnergyChem* **2022**, *4*, 100075. [[CrossRef](#)]
82. Musiał, M.; Malarz, K.; Mrozek-Wilczkiewicz, A.; Musiol, R.; Zorębski, E.; Dzida, M. Pyrrolidinium-Based Ionic Liquids as Sustainable Media in Heat-Transfer Processes. *ACS Sustain. Chem. Eng.* **2017**, *5*, 11024–11033. [[CrossRef](#)]
83. Jamil, R.; Loomba, S.; Kar, M.; Collis, G.E.; Sylvester, D.S.; Mahmood, N. Metal Anodes Meet Ionic Liquids: An Interfacial Perspective. *Appl. Phys. Rev.* **2024**, *11*, 011307. [[CrossRef](#)]
84. Ma, L.A.; Naylor, A.J.; Nyholm, L.; Younesi, R. Strategies for Mitigating Dissolution of Solid Electrolyte Interphases in Sodium-Ion Batteries. *Angew. Chem. Int. Ed.* **2021**, *60*, 4855–4863. [[CrossRef](#)]
85. Mogensen, R.; Brandell, D.; Younesi, R. Solubility of the Solid Electrolyte Interphase (SEI) in Sodium Ion Batteries. *ACS Energy Lett.* **2016**, *1*, 1173–1178. [[CrossRef](#)]
86. Bao, C.; Wang, B.; Liu, P.; Wu, H.; Zhou, Y.; Wang, D.; Liu, H.; Dou, S.; Bao, C.Y.; Wang, B.; et al. Solid Electrolyte Interphases on Sodium Metal Anodes. *Adv. Funct. Mater.* **2020**, *30*, 2004891. [[CrossRef](#)]

87. Zhu, C.; Wu, D.; Wang, Z.; Wang, H.; Liu, J.; Guo, K.; Liu, Q.; Ma, J.; Zhu, C.; Wu, D.; et al. Optimizing NaF-Rich Solid Electrolyte Interphase for Stabilizing Sodium Metal Batteries by Electrolyte Additive. *Adv. Funct. Mater.* **2024**, *34*, 2214195. [CrossRef]
88. Lin, Y.; Peng, Q.; Chen, L.; Zuo, Q.; Long, Q.; Lu, F.; Huang, S.; Chen, Y.; Meng, Y. Organic Liquid Electrolytes in Sodium-Based Batteries: Actualities and Perspectives. *Energy Storage Mater.* **2024**, *67*, 103211. [CrossRef]
89. Li, K.; Zhang, J.; Lin, D.; Wang, D.W.; Li, B.; Lv, W.; Sun, S.; He, Y.B.; Kang, F.; Yang, Q.H.; et al. Evolution of the Electrochemical Interface in Sodium Ion Batteries with Ether Electrolytes. *Nat. Commun.* **2019**, *10*, 725. [CrossRef]
90. Cui, R.; Ma, Y.; Gao, X.; Wang, W.; Wang, J.; Xing, Z.; Ju, Z. Research Progress of Co-Intercalation Mechanism Electrolytes in Sodium-Ion Batteries. *Energy Storage Mater.* **2024**, *71*, 103627. [CrossRef]
91. Cheng, F.; Cao, M.; Li, Q.; Fang, C.; Han, J.; Huang, Y. Electrolyte Salts for Sodium-Ion Batteries: NaPF₆ or NaClO₄? *ACS Nano* **2023**, *17*, 18608–18615. [CrossRef]
92. Barnes, P.; Smith, K.; Parrish, R.; Jones, C.; Skinner, P.; Storch, E.; White, Q.; Deng, C.; Karsann, D.; Lau, M.L.; et al. A Non-Aqueous Sodium Hexafluorophosphate-Based Electrolyte Degradation Study: Formation and Mitigation of Hydrofluoric Acid. *J. Power Sources* **2020**, *447*, 227363. [CrossRef]
93. Ponrouch, A.; Monti, D.; Boschin, A.; Steen, B.; Johansson, P.; Palacín, M.R. Non-Aqueous Electrolytes for Sodium-Ion Batteries. *J. Mater. Chem. A Mater.* **2014**, *3*, 22–42. [CrossRef]
94. Seki, S.; Kobayashi, T.; Kobayashi, Y.; Takei, K.; Miyashiro, H.; Hayamizu, K.; Suzuki, S.; Mitsugi, T.; Umebayashi, Y. Effects of Cation and Anion on Physical Properties of Room-Temperature Ionic Liquids. *J. Mol. Liq.* **2010**, *152*, 9–13. [CrossRef]
95. Eshetu, G.G.; Elia, G.A.; Armand, M.; Forsyth, M.; Komaba, S.; Rojo, T.; Passerini, S. Electrolytes and Interphases in Sodium-Based Rechargeable Batteries: Recent Advances and Perspectives. *Adv. Energy Mater.* **2020**, *10*, 2000093. [CrossRef]
96. Wang, B.; Qin, L.; Mu, T.; Xue, Z.; Gao, G. Are Ionic Liquids Chemically Stable? *Chem. Rev.* **2017**, *117*, 7113–7131. [CrossRef] [PubMed]
97. Galiński, M.; Lewandowski, A.; Stepniak, I. Ionic Liquids as Electrolytes. *Electrochim. Acta* **2006**, *51*, 5567–5580. [CrossRef]
98. Xue, Z.; Qin, L.; Jiang, J.; Mu, T.; Gao, G. Thermal, Electrochemical and Radiolytic Stabilities of Ionic Liquids. *Phys. Chem. Chem. Phys.* **2018**, *20*, 8382–8402. [CrossRef]
99. Ding, C.; Nohira, T.; Hagiwara, R.; Matsumoto, K.; Okamoto, Y.; Fukunaga, A.; Sakai, S.; Nitta, K.; Inazawa, S. Na[FSAs]-[C3C1pyrr][FSA] Ionic Liquids as Electrolytes for Sodium Secondary Batteries: Effects of Na Ion Concentration and Operation Temperature. *J. Power Sources* **2014**, *269*, 124–128. [CrossRef]
100. Hilder, M.; Howlett, P.C.; Saurel, D.; Gonzalo, E.; Basile, A.; Armand, M.; Rojo, T.; Kar, M.; MacFarlane, D.R.; Forsyth, M. The Effect of Cation Chemistry on Physicochemical Behaviour of Superconcentrated NaFSI Based Ionic Liquid Electrolytes and the Implications for Na Battery Performance. *Electrochim. Acta* **2018**, *268*, 94–100. [CrossRef]
101. Golding, J.; Hamid, N.; MacFarlane, D.R.; Forsyth, M.; Forsyth, C.; Collins, C.; Huang, J. N-Methyl-N-Alkylpyrrolidinium Hexafluorophosphate Salts: Novel Molten Salts and Plastic Crystal Phases. *Chem. Mater.* **2001**, *13*, 558–564. [CrossRef]
102. Harris, K.R.; Woolf, L.A.; Kanakubo, M. Temperature and Pressure Dependence of the Viscosity of the Ionic Liquid 1-Butyl-3-Methylimidazolium Hexafluorophosphate. *J. Chem. Eng. Data* **2005**, *50*, 1777–1782. [CrossRef]
103. Wang, D.; Takiyama, M.; Hwang, J.; Matsumoto, K.; Hagiwara, R. A Hexafluorophosphate-Based Ionic Liquid as Multifunctional Interfacial Layer between High Voltage Positive Electrode and Solid-State Electrolyte for Sodium Secondary Batteries. *Adv. Energy Mater.* **2023**, *13*, 2301020. [CrossRef]
104. Plashnitsa, L.S.; Kobayashi, E.; Noguchi, Y.; Okada, S.; Yamaki, J. Performance of NASICON Symmetric Cell with Ionic Liquid Electrolyte. *J. Electrochem. Soc.* **2010**, *157*, A536. [CrossRef]
105. Wu, F.; Zhu, N.; Bai, Y.; Liu, L.; Zhou, H.; Wu, C. Highly Safe Ionic Liquid Electrolytes for Sodium-Ion Battery: Wide Electrochemical Window and Good Thermal Stability. *ACS Appl. Mater. Interfaces* **2016**, *8*, 21381–21386. [CrossRef] [PubMed]
106. Fischer, P.J.; Do, M.P.; Reich, R.M.; Nagasubramanian, A.; Srinivasan, M.; Kühn, F.E. Synthesis and Physicochemical Characterization of Room Temperature Ionic Liquids and Their Application in Sodium Ion Batteries. *Phys. Chem. Chem. Phys.* **2018**, *20*, 29412–29422. [CrossRef] [PubMed]
107. Bazito, F.F.C.; Kawano, Y.; Torresi, R.M. Synthesis and Characterization of Two Ionic Liquids with Emphasis on Their Chemical Stability towards Metallic Lithium. *Electrochim. Acta* **2007**, *52*, 6427–6437. [CrossRef]
108. Hosokawa, T.; Matsumoto, K.; Nohira, T.; Hagiwara, R.; Fukunaga, A.; Sakai, S.; Nitta, K. Stability of Ionic Liquids against Sodium Metal: A Comparative Study of 1-Ethyl-3-Methylimidazolium Ionic Liquids with Bis(Fluorosulfonyl)Amide and Bis(Trifluoromethylsulfonyl)Amide. *J. Phys. Chem. C* **2016**, *120*, 9628–9636. [CrossRef]
109. Wibowo, R.; Aldous, L.; Rogers, E.I.; Ward Jones, S.E.; Compton, R.G. A Study of the Na/Na⁺ Redox Couple in Some Room Temperature Ionic Liquids. *J. Phys. Chem. C* **2010**, *114*, 3618–3626. [CrossRef]
110. Wu, S.; Wada, T.; Shionoya, H.; Hwang, J.; Matsumoto, K.; Hagiwara, R. Practical Level of Low-N/P Ratio Sodium Metal Batteries: On the Basis of Deposition/Dissolution Efficiency in the Aspects of Electrolytes and Temperature. *Energy Storage Mater.* **2023**, *61*, 102897. [CrossRef]

111. Ding, C.; Nohira, T.; Kuroda, K.; Hagiwara, R.; Fukunaga, A.; Sakai, S.; Nitta, K.; Inazawa, S. NaFSA-C₁C₃pyrFSA Ionic Liquids for Sodium Secondary Battery Operating over a Wide Temperature Range. *J. Power Sources* **2013**, *238*, 296–300. [CrossRef]
112. Basile, A.; Makhlooghiyazad, F.; Yunis, R.; MacFarlane, D.R.; Forsyth, M.; Howlett, P.C. Extensive Sodium Metal Plating and Stripping in a Highly Concentrated Inorganic–Organic Ionic Liquid Electrolyte through Surface Pretreatment. *ChemElectroChem* **2017**, *4*, 986–991. [CrossRef]
113. Basile, A.; Ferdousi, S.A.; Makhlooghiyazad, F.; Yunis, R.; Hilder, M.; Forsyth, M.; Howlett, P.C. Beneficial Effect of Added Water on Sodium Metal Cycling in Super Concentrated Ionic Liquid Sodium Electrolytes. *J. Power Sources* **2018**, *379*, 344–349. [CrossRef]
114. Ferdousi, S.A.; O’Dell, L.A.; Hilder, M.; Barlow, A.J.; Armand, M.; Forsyth, M.; Howlett, P.C. SEI Formation on Sodium Metal Electrodes in Superconcentrated Ionic Liquid Electrolytes and the Effect of Additive Water. *ACS Appl. Mater. Interfaces* **2021**, *13*, 5706–5720. [CrossRef]
115. Sun, J.; Rakov, D.; Wang, J.; Hora, Y.; Laghaei, M.; Byrne, N.; Wang, X.; Howlett, P.C.; Forsyth, M. Sustainable Free-Standing Electrode from Biomass Waste for Sodium-Ion Batteries. *ChemElectroChem* **2022**, *9*, e202200382. [CrossRef]
116. Sun, J.; O’Dell, L.A.; Armand, M.; Howlett, P.C.; Forsyth, M. Anion-Derived Solid-Electrolyte Interphase Enables Long Life Na-Ion Batteries Using Superconcentrated Ionic Liquid Electrolytes. *ACS Energy Lett.* **2021**, *6*, 2481–2490. [CrossRef]
117. Wongittharom, N.; Wang, C.H.; Wang, Y.C.; Yang, C.H.; Chang, J.K. Ionic Liquid Electrolytes with Various Sodium Solutes for Rechargeable Na/NaFePO₄ Batteries Operated at Elevated Temperatures. *ACS Appl. Mater. Interfaces* **2014**, *6*, 17564–17570. [CrossRef] [PubMed]
118. Chen, C.Y.; Matsumoto, K.; Nohira, T.; Hagiwara, R.; Orikasa, Y.; Uchimoto, Y. Pyrophosphate Na₂FeP₂O₇ as a Low-Cost and High-Performance Positive Electrode Material for Sodium Secondary Batteries Utilizing an Inorganic Ionic Liquid. *J. Power Sources* **2014**, *246*, 783–787. [CrossRef]
119. Oh, J.A.S.; He, H.; Sun, J.; Cao, X.; Chua, B.; Huang, Y.; Zeng, K.; Lu, L. Dual-Nitrogen-Doped Carbon Decorated on Na₃V₂(PO₄)₃ to Stabilize the Intercalation of Three Sodium Ions. *ACS Appl. Energy Mater.* **2020**, *3*, 6870–6879. [CrossRef]
120. Ding, C.; Nohira, T.; Hagiwara, R. Charge-Discharge Performance of Na_{2/3}Fe_{1/3}Mn_{2/3}O₂ Positive Electrode in an Ionic Liquid Electrolyte at 90 °C for Sodium Secondary Batteries. *Electrochim. Acta* **2017**, *231*, 412–416. [CrossRef]
121. Hasa, I.; Passerini, S.; Hassoun, J. Characteristics of an Ionic Liquid Electrolyte for Sodium-Ion Batteries. *J. Power Sources* **2016**, *303*, 203–207.
122. Wang, X.; Shang, Z.; Yang, A.; Zhang, Q.; Cheng, F.; Jia, D.; Chen, J. Combining Quinone Cathode and Ionic Liquid Electrolyte for Organic Sodium-Ion Batteries. *Chem* **2019**, *5*, 364–375. [CrossRef]
123. Forsyth, M.; Yoon, H.; Chen, F.; Zhu, H.; MacFarlane, D.R.; Armand, M.; Howlett, P.C. Novel Na⁺ Ion Diffusion Mechanism in Mixed Organic-Inorganic Ionic Liquid Electrolyte Leading to High Na⁺ Transference Number and Stable, High Rate Electrochemical Cycling of Sodium Cells. *J. Phys. Chem. C* **2016**, *120*, 4276–4286. [CrossRef]
124. Matsumoto, K.; Okamoto, Y.; Nohira, T.; Hagiwara, R. Thermal and Transport Properties of Na[N(SO₂F)₂]-[N-Methyl-N-Propylpyrrolidinium][N(SO₂F)₂] Ionic Liquids for Na Secondary Batteries. *J. Phys. Chem. C* **2015**, *119*, 7648–7655. [CrossRef]
125. Massaro, A.; Lingua, G.; Bozza, F.; Piovano, A.; Prosini, P.P.; Muñoz-García, A.B.; Pavone, M.; Gerbaldi, C. P2-Type Na_{0.84}Li_{0.1}Ni_{0.27}Mn_{0.63}O₂-Layered Oxide Na-Ion Battery Cathode: Structural Insights and Electrochemical Compatibility with Room-Temperature Ionic Liquids. *Chem. Mater.* **2024**, *36*, 7046–7055. [CrossRef] [PubMed]
126. Do, M.P.; Bucher, N.; Nagasubramanian, A.; Markovits, I.; Bingbing, T.; Fischer, P.J.; Loh, K.P.; Kühn, F.E.; Srinivasan, M. Effect of Conducting Salts in Ionic Liquid Electrolytes for Enhanced Cyclability of Sodium-Ion Batteries. *ACS Appl. Mater. Interfaces* **2019**, *11*, 23972–23981. [CrossRef] [PubMed]
127. Wu, F.; Zhu, N.; Bai, Y.; Li, Y.; Wang, Z.; Ni, Q.; Wang, H.; Wu, C. Unveil the Mechanism of Solid Electrolyte Interphase on Na₃V₂(PO₄)₃ Formed by a Novel NaPF₆/BMITFSI Ionic Liquid Electrolyte. *Nano Energy* **2018**, *51*, 524–532. [CrossRef]
128. Chagas, L.G.; Jeong, S.; Hasa, I.; Passerini, S. Ionic Liquid-Based Electrolytes for Sodium-Ion Batteries: Tuning Properties to Enhance the Electrochemical Performance of Manganese-Based Layered Oxide Cathode. *ACS Appl. Mater. Interfaces* **2019**, *11*, 22278–22289. [CrossRef]
129. Hilder, M.; Gras, M.; Pope, C.R.; Kar, M.; Macfarlane, D.R.; Forsyth, M.; O’Dell, L.A. Effect of Mixed Anions on the Physicochemical Properties of a Sodium Containing Alkoxyammonium Ionic Liquid Electrolyte. *Phys. Chem. Chem. Phys.* **2017**, *19*, 17461–17468. [CrossRef]
130. Hosseini-Bab-Anari, E.; Navarro-Suárez, A.M.; Moth-Poulsen, K.; Johansson, P. Ionic Liquid Based Battery Electrolytes Using Lithium and Sodium Pseudo-Delocalized Pyridinium Anion Salts. *Phys. Chem. Chem. Phys.* **2019**, *21*, 18393–18399. [CrossRef]
131. Maresca, G.; Ottaviani, M.; Ryan, K.M.; Brutti, S.; Appetecchi, G.B. Physicochemical Investigation on the Hard Carbon Interface in Ionic Liquid Electrolyte. *Electrochim. Acta* **2024**, *498*, 144631. [CrossRef]
132. Chagas, L.G.; Buchholz, D.; Wu, L.; Vortmann, B.; Passerini, S. Unexpected Performance of Layered Sodium-Ion Cathode Material in Ionic Liquid-Based Electrolyte. *J. Power Sources* **2014**, *247*, 377–383. [CrossRef]

133. Forsyth, M.; Hilder, M.; Zhang, Y.; Chen, F.; Carre, L.; Rakov, D.A.; Armand, M.; Macfarlane, D.R.; Pozo-Gonzalo, C.; Howlett, P.C. Tuning Sodium Interfacial Chemistry with Mixed-Anion Ionic Liquid Electrolytes. *ACS Appl. Mater. Interfaces* **2019**, *11*, 43093–43106. [[CrossRef](#)]
134. Basile, A.; Yoon, H.; MacFarlane, D.R.; Forsyth, M.; Howlett, P.C. Investigating Non-Fluorinated Anions for Sodium Battery Electrolytes Based on Ionic Liquids. *Electrochim. Commun.* **2016**, *71*, 48–51. [[CrossRef](#)]
135. Sun, H.; Zhu, G.; Xu, X.; Liao, M.; Li, Y.Y.; Angell, M.; Gu, M.; Zhu, Y.; Hung, W.H.; Li, J.; et al. A Safe and Non-Flammable Sodium Metal Battery Based on an Ionic Liquid Electrolyte. *Nat. Commun.* **2019**, *10*, 3302. [[CrossRef](#)] [[PubMed](#)]
136. Lee, S.; Koo, B.; Kang, S.; Lee, H.; Lee, H. Hydrofluoroether-Assisted Dilution of Na-Ion Concentrated Ionic Liquid Electrolyte for Safe, Stable Cycling of High-Voltage Na-Metal Batteries. *Chem. Eng. J.* **2021**, *425*, 130612. [[CrossRef](#)]
137. Noor, S.A.M.; Su, N.C.; Khoon, L.T.; Mohamed, N.S.; Ahmad, A.; Yahya, M.Z.A.; Zhu, H.; Forsyth, M.; MacFarlane, D.R. Properties of High Na-Ion Content N-Propyl-N-Methylpyrrolidinium Bis(Fluorosulfonyl)Imide -Ethylene Carbonate Electrolytes. *Electrochim. Acta* **2017**, *247*, 983–993. [[CrossRef](#)]
138. Quan, P.; Linh, L.T.M.; Tuyen, H.T.K.; Van Hoang, N.; Thanh, V.D.; Van Man, T.; Phung, L.M.L. Safe Sodium-Ion Battery Using Hybrid Electrolytes of Organic Solvent/Pyrrolidinium Ionic Liquid. *Vietnam. J. Chem.* **2021**, *59*, 17–26. [[CrossRef](#)]
139. Benchakar, M.; Naéjus, R.; Damas, C.; Santos-Peña, J. Exploring the Use of EMImFSI Ionic Liquid as Additive or Co-Solvent for Room Temperature Sodium Ion Battery Electrolytes. *Electrochim. Acta* **2020**, *330*, 135193. [[CrossRef](#)]
140. Arkhipova, E.A.; Levin, M.M.; Ivanov, A.S.; Zakharov, M.A.; Kozhatkin, I.D.; Maslakov, K.I.; Singh, P.K.; Savilov, S.V. Electroactive Ferrocene-Based Ionic Liquids: Transport and Electrochemical Properties of Their Acetonitrile Solutions. *Electrochim. Acta* **2025**, *512*, 145443. [[CrossRef](#)]
141. Zhang, T.; Wang, Y.; Song, T.; Miyaoka, H.; Shinzato, K.; Miyaoka, H.; Ichikawa, T.; Shi, S.; Zhang, X.; Isobe, S.; et al. Ammonia, a Switch for Controlling High Ionic Conductivity in Lithium Borohydride Ammoniates. *Joule* **2018**, *2*, 1522–1533. [[CrossRef](#)]
142. Yan, Y.; Grinderslev, J.B.; Lee, Y.S.; Jørgensen, M.; Cho, Y.W.; Černý, R.; Jensen, T.R. Ammonia-Assisted Fast Li-Ion Conductivity in a New Hemiammine Lithium Borohydride, LiBH₄·1/2NH₃. *Chem. Commun.* **2020**, *56*, 3971–3974. [[CrossRef](#)]
143. Kraus, F.; Fichtl, M.B.; Baer, S.A. Beryllium Diammine Difluoride [BeF₂(NH₃)₂]. *Z. Fur Naturforschung—Sect. B J. Chem. Sci.* **2009**, *64*, 257–262. [[CrossRef](#)]
144. Goncalves, A.; Tran-Van, P.; Herlem, G.; Kwa, E.; Fahys, B.; Herlem, M. New Potential Candidates for Redox Battery Using Liquid Ammoniates: Na⁺/Na and Ag⁺/Ag. *Port. Electrochim. Acta* **2006**, *26*, 117–127.
145. Badoz-Lambling, J.; Bardin, M.; Bernard, C.; Fahys, B.; Herlem, M.; Thiebault, A.; Robert, G. New Battery Electrolytes for Low and High Temperatures: Liquid and Solid Ammoniates for High Energy Batteries I. Sodium Iodide and Lithium Perchlorate Ammoniates. *Electrochim. Soc.* **1988**, *135*, 587.
146. Ruiz-Martínez, D.; Kovacs, A.; Gómez, R. Development of Novel Inorganic Electrolytes for Room Temperature Rechargeable Sodium Metal Batteries. *Energy Environ. Sci.* **2017**, *10*, 1936–1941. [[CrossRef](#)]
147. Geng, C.; Buchholz, D.; Kim, G.T.; Carvalho, D.V.; Zhang, H.; Chagas, L.G.; Passerini, S. Influence of Salt Concentration on the Properties of Sodium-Based Electrolytes. *Small Methods* **2019**, *3*, 1800208. [[CrossRef](#)]
148. Song, B.; Xiong, X.; Peng, Y.; Liu, X.; Gao, W.; Wang, T.; Wang, F.; Ma, Y.; Zhong, Y.; Cheng, X.B.; et al. Review of Electrolyte Additives for Secondary Sodium Batteries. *Adv. Energy Mater.* **2024**, *14*, 2401407.
149. Tapia-Ruiz, N.; Armstrong, A.R.; Alptekin, H.; Amores, M.A.; Au, H.; Barker, J.; Boston, R.; Brant, W.R.; Brittain, J.M.; Chen, Y.; et al. 2021 Roadmap for Sodium-Ion Batteries. *J. Phys. Energy* **2021**, *3*, 31503. [[CrossRef](#)]
150. Wei Seh, Z.; Sun, J.; Sun, Y.; Cui, Y. A Highly Reversible Room-Temperature Sodium Metal Anode. *ACS Cent. Sci.* **2015**, *1*, 449–455. [[CrossRef](#)]
151. Yang, Z.; He, J.; Lai, W.-H.; Peng, J.; Liu, X.-H.; He, X.-X.; Guo, X.-F.; Li, L.; Qiao, Y.; Ma, J.-M.; et al. Fire-Retardant, Stable-Cycling and High-Safety Sodium Ion Battery. *Angew. Chem.* **2021**, *133*, 27292–27300. [[CrossRef](#)]
152. Lu, L.; Han, X.; Li, J.; Hua, J.; Ouyang, M. A Review on the Key Issues for Lithium-Ion Battery Management in Electric Vehicles. *J. Power Sources* **2013**, *226*, 272–288. [[CrossRef](#)]
153. Wang, Y.; Ou, R.; Yang, J.; Xin, Y.; Singh, P.; Wu, F.; Qian, Y.; Gao, H. The Safety Aspect of Sodium Ion Batteries for Practical Applications. *J. Energy Chem.* **2024**, *95*, 407–427. [[CrossRef](#)]
154. Yamada, Y.; Wang, J.; Ko, S.; Watanabe, E.; Yamada, A. Advances and Issues in Developing Salt-Concentrated Battery Electrolytes. *Nat. Energy* **2019**, *4*, 269–280.
155. Ye, Z.; Li, J.; Li, Z. Recent Progress in Nonflammable Electrolytes and Cell Design for Safe Li-Ion Batteries. *J. Mater. Chem. A Mater.* **2023**, *11*, 15576–15599. [[CrossRef](#)]
156. Gond, R.; Van Ekeren, W.; Mogensen, R.; Naylor, A.J.; Younesi, R. Non-Flammable Liquid Electrolytes for Safe Batteries. *Mater. Horiz.* **2021**, *8*, 2913–2928. [[CrossRef](#)] [[PubMed](#)]
157. Herlem, M.; Székely, M.; Sutter, E.; Mathieu, C.; Gonçalves, A.M.; Caillot, E.; Herlem, G.; Fahys, B. Liquid Ammoniates: Nonaqueous Electrolytes for Electrochromism. *Electrochim. Acta* **2001**, *46*, 2967–2973. [[CrossRef](#)]

158. Yan, T.; Wang, R.Z.; Li, T.X.; Wang, L.W.; Fred, I.T. A Review of Promising Candidate Reactions for Chemical Heat Storage. *Renew. Sustain. Energy Rev.* **2015**, *43*, 13–31. [[CrossRef](#)]
159. Fujiwara, I.; Nakashima, Y.; Goto, T. Thermal energy storage with chemical reaction of NaI/NH₃ system-I. Region of liquid phase. *Energy Convers. Manag.* **1981**, *21*, 157–162. [[CrossRef](#)]
160. Osman, A.I.; Nasr, M.; Eltaweil, A.S.; Hosny, M.; Farghali, M.; Al-Fatesh, A.S.; Rooney, D.W.; Abd El-Monaem, E.M. Advances in Hydrogen Storage Materials: Harnessing Innovative Technology, from Machine Learning to Computational Chemistry, for Energy Storage Solutions. *Int. J. Hydrot. Energy* **2024**, *67*, 1270–1294. [[CrossRef](#)]
161. Vittetoe, A.W.; Niemann, M.U.; Srinivasan, S.S.; McGrath, K.; Kumar, A.; Goswami, D.Y.; Stefanakos, E.K.; Thomas, S. Destabilization of LiAlH₄ by Nanocrystalline MgH₂. *Int. J. Hydrot. Energy* **2009**, *34*, 2333–2339. [[CrossRef](#)]
162. Iosub, V.; Matsunaga, T.; Tange, K.; Ishikiriyama, M. Direct Synthesis of Mg(AlH₄)₂ and CaAlH₅ Crystalline Compounds by Ball Milling and Their Potential as Hydrogen Storage Materials. *Int. J. Hydrot. Energy* **2009**, *34*, 906–912. [[CrossRef](#)]
163. Srinivasan, S.; Escobar, D.; Goswami, Y.; Stefanakos, E. Effects of Catalysts Doping on the Thermal Decomposition Behavior of Zn(BH₄)₂. *Int. J. Hydrot. Energy* **2008**, *33*, 2268–2272. [[CrossRef](#)]
164. Arnbjerg, L.M.; Ravnsbæk, D.B.; Filinchuk, Y.; Vang, R.T.; Cerenius, Y.; Besenbacher, F.; Jørgensen, J.E.; Jakobsen, H.J.; Jensen, T.R. Structure and Dynamics for LiBH₄—LiCl Solid Solutions. *Chem. Mater.* **2009**, *21*, 5772–5782. [[CrossRef](#)]
165. Bogdanović, B.; Felderhoff, M.; Streukens, G. Hydrogen Storage in Complex Metal Hydrides[Russian Source]. *J. Serbian Chem. Soc.* **2009**, *74*, 183–196. [[CrossRef](#)]
166. Demirci, U.B. Ammonia Borane, a Material with Exceptional Properties for Chemical Hydrogen Storage. *Int. J. Hydrot. Energy* **2017**, *42*, 9978–10013. [[CrossRef](#)]
167. Züttel, A.; Wenger, P.; Rentsch, S.; Sudan, P.; Mauron, P.; Emmenegger, C. LiBH₄ a New Hydrogen Storage Material. *J. Power Sources* **2003**, *118*, 1–7. [[CrossRef](#)]
168. Vajo, J.J.; Skeith, S.L.; Mertens, F. Reversible Storage of Hydrogen in Destabilized LiBH₄. *J. Phys. Chem. B* **2005**, *109*, 3719–3722. [[CrossRef](#)]
169. Guo, Y.; Xia, G.; Zhu, Y.; Gao, L.; Yu, X. Hydrogen Release from Ammine lithium Borohydride, LiBH₄·NH₃. *Chem. Commun.* **2010**, *46*, 2599–2601. [[CrossRef](#)]
170. Soloveichik, G.; Her, J.H.; Stephens, P.W.; Gao, Y.; Rijssenbeek, J.; Andrus, M.; Zhao, J.C. Ammine Magnesium Borohydride Complex as a New Material for Hydrogen Storage: Structure and Properties of Mg(BH₄)₂·2NH₃. *Inorg. Chem.* **2008**, *47*, 4290–4298. [[CrossRef](#)]
171. Chua, Y.S.; Wu, G.; Xiong, Z.; He, T.; Chen, P. Calcium Amidoborane Ammoniate-Synthesis, Structure, and Hydrogen Storage Properties. *Chem. Mater.* **2009**, *21*, 4899–4904. [[CrossRef](#)]
172. Tang, Z.; Tan, Y.; Wu, H.; Gu, Q.; Zhou, W.; Jensen, C.M.; Yu, X. Metal Cation-Promoted Hydrogen Generation in Activated Aluminium Borohydride Ammoniates. *Acta Mater.* **2013**, *61*, 4787–4796. [[CrossRef](#)]
173. Zheng, X.; Wu, G.; Li, W.; Xiong, Z.; He, T.; Guo, J.; Chen, H.; Chen, P. Releasing 17.8 Wt% H₂ from Lithium Borohydride Ammoniate. *Energy Environ. Sci.* **2011**, *4*, 3593–3600. [[CrossRef](#)]
174. Wang, M.; Ouyang, L.; Peng, C.; Zhu, X.; Zhu, W.; Shao, H.; Zhu, M. Synthesis and Hydrolysis of NaZn(BH₄)₃ and Its Ammoniates. *J. Mater. Chem. A Mater.* **2017**, *5*, 17012–17020. [[CrossRef](#)]
175. Guo, Y.; Wu, H.; Zhou, W.; Yu, X. Dehydrogenation Tuning of Ammine Borohydrides Using Double-Metal Cations. *J. Am. Chem. Soc.* **2011**, *133*, 4690–4693. [[CrossRef](#)] [[PubMed](#)]
176. Xia, G.; Gu, Q.; Guo, Y.; Yu, X. Ammine Bimetallic (Na, Zn) Borohydride for Advanced Chemical Hydrogen Storage. *J. Mater. Chem.* **2012**, *22*, 7300–7307. [[CrossRef](#)]
177. Divers, E., IX. On the Union of Ammonia Nitrate with Ammonia. *Philos. Trans. R. Soc. Lond.* **1873**, *163*, 359–376.
178. Ruiz-Martínez, D.; Gómez, R. The Liquid Ammoniate of Sodium Iodide as an Alternative Electrolyte for Sodium Ion Batteries: The Case of Titanium Dioxide Nanotube Electrodes. *Energy Storage Mater.* **2019**, *22*, 424–432. [[CrossRef](#)]
179. Ruiz-Martínez, D.; Orts, J.M.; Gómez, R. A Stable Anthraquinone-Derivative Cathode to Develop Sodium Metal Batteries: The Role of Ammoniates as Electrolytes. *J. Energy Chem.* **2023**, *77*, 572–580. [[CrossRef](#)]
180. Ruiz-Martínez, D.; Lana-Villarreal, T.; Gómez, R. Liquid Ammoniates as Efficient Electrolytes for Room-Temperature Rechargeable Sodium-Metal Batteries Based on an Organic Cathode. *ACS Appl. Energy Mater.* **2021**, *4*, 6806–6814. [[CrossRef](#)]
181. Fahys, B.; Herlem, M. Lithium Nitrate and Lithium Trifluoromethanesulfonate Ammoniates for Electrolytes in Lithium Batteries. *J. Power Sources* **1991**, *34*, 183–188. [[CrossRef](#)]
182. Fahys, B.R.; Herlem, M.P.; Jaume, J. New Electrolytes from Concentrated Solutions of Lithium Salts in Mixtures of Ammonia And Amines. *Electrochim. Acta* **1994**, *39*, 2343–2346. [[CrossRef](#)]
183. Xie, Z.; Wu, Z.; An, X.; Yue, X.; Wang, J.; Abudula, A.; Guan, G. Anode-Free Rechargeable Lithium Metal Batteries: Progress and Prospects. *Energy Storage Mater.* **2020**, *32*, 386–401. [[CrossRef](#)]
184. Genovese, M.; Louli, A.J.; Weber, R.; Hames, S.; Dahn, J.R. Measuring the Coulombic Efficiency of Lithium Metal Cycling in Anode-Free Lithium Metal Batteries. *J. Electrochem. Soc.* **2018**, *165*, A3321–A3325. [[CrossRef](#)]

185. Hu, Z.; Liu, L.; Wang, X.; Zheng, Q.; Han, C.; Li, W. Current Progress of Anode-Free Rechargeable Sodium Metal Batteries: Origin, Challenges, Strategies, and Perspectives. *Adv. Funct. Mater.* **2024**, *34*, 2313823.
186. Cohn, A.P.; Muralidharan, N.; Carter, R.; Share, K.; Pint, C.L. Anode-Free Sodium Battery through in Situ Plating of Sodium Metal. *Nano Lett.* **2017**, *17*, 1296–1301. [CrossRef] [PubMed]
187. Tian, Y.; An, Y.; Wei, C.; Jiang, H.; Xiong, S.; Feng, J.; Qian, Y. Recently Advances and Perspectives of Anode-Free Rechargeable Batteries. *Nano Energy* **2020**, *78*, 105344.
188. Zhang, H.; Gao, Y.; Liu, X.H.; Yang, Z.; He, X.X.; Li, L.; Qiao, Y.; Chen, W.H.; Zeng, R.H.; Wang, Y.; et al. Organic Cathode Materials for Sodium-Ion Batteries: From Fundamental Research to Potential Commercial Application. *Adv. Funct. Mater.* **2022**, *32*, 2107718.
189. Han, H.; Lu, H.; Jiang, X.; Zhong, F.; Ai, X.; Yang, H.; Cao, Y. Polyaniline Hollow Nanofibers Prepared by Controllable Sacrifice-Template Route as High-Performance Cathode Materials for Sodium-Ion Batteries. *Electrochim. Acta* **2019**, *301*, 352–358. [CrossRef]
190. Wu, Y.; Chen, Y.; Tang, M.; Zhu, S.; Jiang, C.; Zhuo, S.; Wang, C. A Highly Conductive Conjugated Coordination Polymer for Fast-Charge Sodium-Ion Batteries: Reconsidering Its Structures. *Chem. Commun.* **2019**, *55*, 10856–10859. [CrossRef]
191. Tang, W.; Liang, R.; Li, D.; Yu, Q.; Hu, J.; Cao, B.; Fan, C. Highly Stable and High Rate-Performance Na-Ion Batteries Using Polyanionic Anthraquinone as the Organic Cathode. *ChemSusChem* **2019**, *12*, 2181–2185. [CrossRef]
192. Yuan, C.; Wu, Q.; Shao, Q.; Li, Q.; Gao, B.; Duan, Q.; Wang, H.G. Free-Standing and Flexible Organic Cathode Based on Aromatic Carbonyl Compound/Carbon Nanotube Composite for Lithium and Sodium Organic Batteries. *J. Colloid. Interface Sci.* **2018**, *517*, 72–79. [CrossRef]
193. Ruiz-Martinez, D.; Grieco, R.; Liras, M.; Patil, N.; Marcilla, R. A High Performing Conjugated Microporous Polymer Cathode for Practical Sodium Metal Batteries Using an Ammoniate as Electrolyte. *Adv. Energy Mater.* **2024**, *14*, 2400857. [CrossRef]
194. Zhang, R.; Zhao, W.; Liu, Z.; Wei, S.; Yan, Y.; Chen, Y. Enhanced Room Temperature Ionic Conductivity of the $\text{LiBH}_4 \cdot 1/2\text{NH}_3\text{-Al}_2\text{O}_3$ composite. *Chem. Commun.* **2021**, *57*, 2380–2383. [CrossRef]
195. Zhao, W.; Zhang, R.; Li, H.; Zhang, Y.; Wang, Y.; Wu, C.; Yan, Y.; Chen, Y. Li-Ion Conductivity Enhancement of $\text{LiBH}_4 \text{XNH}_3$ with In Situ Formed Li_2O Nanoparticles. *ACS Appl. Mater. Interfaces* **2021**, *13*, 31635–31641. [CrossRef] [PubMed]
196. Zhang, R.; Li, H.; Wang, Q.; Wei, S.; Yan, Y.; Chen, Y. Size Effect of MgO on the Ionic Conduction Properties of a $\text{LiBH}_4 \cdot 1/2\text{NH}_3\text{-MgO}$ Nanocomposite. *ACS Appl. Mater. Interfaces* **2022**, *14*, 8947–8954. [CrossRef] [PubMed]
197. Liu, Z.; Zhang, T.; Ju, S.; Ji, Y.; Hu, Z.; Lv, Y.; Xia, G.; Yu, X. Fast Ionic Migration from Bulk to Interface in the $\text{Li}(\text{NH}_3) \text{XBH}_4 @ \text{SiO}_2$ Composite. *ACS Appl. Energy Mater.* **2022**, *5*, 14301–14310. [CrossRef]
198. Pang, Y.; Nie, Z.; Xu, F.; Sun, L.; Yang, J.; Sun, D.; Fang, F.; Zheng, S. Borohydride Ammoniate Solid Electrolyte Design for All-Solid-State Mg Batteries. *Energy Environ. Mater.* **2024**, *7*, e12527. [CrossRef]
199. Yan, Y.; Grinderveslev, J.B.; Jorgensen, M.; Skov, L.N.; Skibsted, J.; Jensen, T.R. Ammine Magnesium Borohydride Nanocomposites for All-Solid-State Magnesium Batteries. *ACS Appl. Energy Mater.* **2020**, *3*, 9264–9270. [CrossRef]
200. Yan, Y.; Grinderveslev, J.B.; Burankova, T.; Wei, S.; Embs, J.P.; Skibsted, J.; Jensen, T.R. Fast Room-Temperature Mg^{2+} Conductivity in $\text{Mg}(\text{BH}_4)_2 \cdot 1.6\text{NH}_3\text{-Al}_2\text{O}_3$ Nanocomposites. *J. Phys. Chem. Lett.* **2022**, *13*, 2211–2216. [CrossRef]

Disclaimer/Publisher’s Note: The statements, opinions and data contained in all publications are solely those of the individual author(s) and contributor(s) and not of MDPI and/or the editor(s). MDPI and/or the editor(s) disclaim responsibility for any injury to people or property resulting from any ideas, methods, instructions or products referred to in the content.